



SCHOOL of
GRADUATE STUDIES
EAST TENNESSEE STATE UNIVERSITY

East Tennessee State University
Digital Commons @ East
Tennessee State University

Electronic Theses and Dissertations

Student Works

12-2010

Mosaic Analysis with Double Markers (MADM) as a Method to Map Cell Fates in Adult Mouse Taste Buds.

Preston D. Moore

East Tennessee State University

Follow this and additional works at: <https://dc.etsu.edu/etd>

 Part of the [Developmental Biology Commons](#)

Recommended Citation

Moore, Preston D., "Mosaic Analysis with Double Markers (MADM) as a Method to Map Cell Fates in Adult Mouse Taste Buds." (2010). *Electronic Theses and Dissertations*. Paper 1764. <https://dc.etsu.edu/etd/1764>

This Thesis - Open Access is brought to you for free and open access by the Student Works at Digital Commons @ East Tennessee State University. It has been accepted for inclusion in Electronic Theses and Dissertations by an authorized administrator of Digital Commons @ East Tennessee State University. For more information, please contact digilib@etsu.edu.

Mosaic Analysis with Double Markers (MADM) as a Method to Map Cell Fates in Adult Mouse

Taste Buds

A thesis

presented to

the faculty of the Department of Anatomy and Cell Biology

East Tennessee State University

in partial fulfillment

of the requirements for the degree

Master of Science in Biomedical Sciences

by

Preston D. Moore

December 2010

Dennis M. Defoe, PhD, Chair

Theresa A. Harrison, PhD

Antonio E. Rusinol, PhD

Keywords: Mosaic Analysis with Double Markers, MADM, Fate Mapping, Lineage Tracing, Taste, Taste Bud, Taste Cell, p27

ABSTRACT

Mosaic Analysis with Double Markers (MADM) as a Method to Map Cell Fates in Adult Mouse Taste Buds

by

Preston D. Moore

Taste buds are chemosensory endorgans embedded in the oral epithelium composed of cells that undergo continuous replacement. Mature taste cells live on average 10-14 days and are replaced by new cells when they die. However, the mechanism by which taste cells are produced and integrated into the taste bud as mature taste cells remains unknown. Previous studies approached this issue from either cell cycle gene expression properties or lineage tracing of precursor cells. In our study, we apply a new fate mapping technique that combines these two ideas. This technique, Mosaic Analysis with Double Markers, allows for simultaneous gene knockout and subsequent tracking of single cells. This allows us to study the potency of precursor cells supplying the taste bud while analyzing how gene function regulates the maturation pathway these taste cells take. The following experiments illustrate the initial phase of this investigation.

ACKNOWLEDGMENTS

To my family, I can never thank you all enough for the love and support you have given me throughout this entire process. Without you, I would have never achieved the success I have obtained thus far, nor be remotely close to the person that I am today. Your continuous encouragement has allowed me to believe not only in myself but also that I can accomplish anything I set my mind to.

To Lydia, we both knew that this would be a trying time in our lives, but you have gone out of your way to make what we have together work. Thank you for being not only the one I can count on when I need to get some things off my mind but also my best friend. This marks just another step in our journey together, and I can't wait to see what lies ahead.

To my committee, Dr. Defoe, Dr. Harrison, and Dr. Rusinol, you all took a student with minimal experience in research under your wings and produced the scientist I am today. Your passion for your careers has allowed me to develop a new appreciation for the field of science and an even greater amount of respect for the researchers of today and tomorrow. I want to thank you all for your time, sound advice, willingness to help, and perhaps most importantly, your patience with me over the last few years. I also appreciate your recognition of the goals I was hoping to achieve by entering this program. Though I am not at that point just yet, I feel that his has most definitely advanced me in the right direction.

To our lab technician, Jarrod, your diligence and attention to detail in the lab in unparalleled to any I have seen before. Managing the upkeep of two labs is a daunting task, but you have done this and managed to help me along the way a great deal. I greatly appreciate all of your assistance, and I wish you all the best in your future endeavors.

To my classmates, it has been an absolute pleasure getting to know each and every one of you. While much of our tenure here has been spent in the confines of the lab, our time in the classroom, our outings, and our occasional crossing of paths during the day made the ride all worth the while. I wish you nothing short of success in both the rest of your duration in the program as well as in your postgraduate careers.

CONTENTS

	Page
ABSTRACT.....	2
ACKNOWLEDGMENTS	3
LIST OF FIGURES	7
Chapter	
1. AN INTRODUCTION TO TASTE BUDS	8
2. FUNCTIONAL EXPRESSION OF THE CYCLIN-DEPENDENT KINASE INHIBITOR p27 ^{Kip1} IN TASTE CELLS.....	17
ABSTRACT.....	18
INTRODUCTION	19
MATERIALS AND METHODS.....	21
Mice and Genotyping.....	21
Preparation of Circumvallate Papillae Cleft Cell Dispersions.....	22
Cell Dispersion Triple-Labeling Immunohistochemistry	23
Cell Dispersion p27 ^{Kip1} Co-Expression Immunohistochemistry	24
Confocal Microscopy and Data Analysis	24
RESULTS	25
DISCUSSION.....	31
REFERENCES	32
3. MOSAIC ANALYSIS WITH DOUBLE MARKERS IDENTIFIES TASTE CELL PROGENY IN ADULT MICE	34
ABSTRACT.....	35

INTRODUCTION	36
MATERIALS AND METHODS.....	42
Mice and Genotyping.....	42
Preparation of Circumvallate Papillae Sections.....	44
MADM Immunohistochemistry.....	45
Confocal Microscopy and Data Analysis	46
RESULTS	46
DISCUSSION.....	59
REFERENCES	61
4. FUTURE DIRECTIONS	62
REFERENCES	64
VITA.....	69

LIST OF FIGURES

Figure	Page
1. Possible cell lineage pathways of mature taste cells.....	14
2. Triple-labeled cell clusters from dispersed cell preparations.	26
3. Loss of p27 ^{Kip1} function does not alter relative taste cell subtype populations.	28
4. Co-Expression of p27 ^{Kip1} and individual taste cell type markers in wild-type mice.	30
5. Target vector for MADM knockin mice.....	38
6. Methodology of MADM strategy given Cre-mediated G ₂ recombination events.....	39
7. Methodology of MADM strategy given Cre-mediated G ₀ /G ₁ recombination events.....	41
8. MADM breeding scheme.....	44
9. Fluorescent stereoscopy images visualizing MADM recombination events.....	47
10. GFP and RFP labeled taste cells represents MADM recombination events.....	50
11. GFP and RFP labeled taste cells in mouse expressing K14-Cre recombinase.....	52
12. GFP and RFP labeled taste cells in mice expressing Hprt-Cre recombinase.....	54
13. Type II cells are labeled by MADM in mice expressing the K14-Cre driver.....	50
14. MADM labels taste cells other than Type II in mice expressing the K14-Cre driver.....	58

CHAPTER 1

AN INTRODUCTION TO TASTE BUDS

Taste buds are the sensory endorgans in vertebrates that communicate taste signals via primary afferent nerves. These buds are composed of an organized collection of anywhere from 30-150 taste cells of varying subtypes (Murray 1973) embedded in multiple regions of the oral epithelium in structures called papillae. In the tongue epithelium there are three types of papillae identified by their respective location on the tongue: circumvallate (posterior dorsal surface), foliate (posterior lateral), and fungiform (anterior). The functional taste cells that comprise the bud are generally characterized as elongated and spanning the width of the tongue epithelium along with a few round unspecialized cells at the base of the bud. While it has been known for quite some time that these functional taste cells undergo continuous turnover to replenish the overall taste cell population from the aforementioned basal cell population (Beidler and Smallman 1965, Farbman 1980), the mechanism of this turnover is still not very well understood. Furthermore, the relationship between the tightly regulated mechanism of cell division and the lineage pathways followed from the proliferative basal cell level to mature and functional taste cells remains to be determined.

Individual taste cells undergo continuous turnover in the taste bud; a process that occurs about every 10-14 days (Beidler and Smallman 1965, Conger and Wells 1969, Farman 1980). Once incorporated into the taste bud structure, the taste cells mature into functional transducers of taste signals. Recent advances in the investigation of taste cells include the ability to differentiate individual taste cells into one of four cell types (I-IV) based on their physiological and protein expression properties.

Type I cells have been determined to have a support or glial-like function and make up about half of the composition of the taste bud (Pumplin et al. 1997). Studies have shown that Type I cells can be identified by their expression of membrane proteins NTPDase2, which hydrolyzes extracellular ATP, and GLAST, a transporter of glutamate. The candidacy of ATP and glutamate as neurotransmitters in the taste system indicate that Type I taste cells may have a role in the termination of synaptic transmission. In addition, they are believed to be transducers of salt taste signals (Lawton et al. 2000; Medler et al. 2003; Finger et al. 2005; Bartel et al. 2006; Romanov and Kolesnikov, 2006).

Type II cells comprise about 35% of the taste bud and have a role in the transduction of sweet, bitter, and umami taste signals. These cells have G-protein coupled receptors that transmit the above taste signals and express the channel protein TRPM5 as well as the calcium-signaling proteins PLC β -2 and IP3R3 (Clapp et al. 2001; Miyoshi et al. 2001; Clapp et al. 2004).

The third and final taste cell type known to have a function in taste signaling, the Type III cells, are the only cells in the taste buds to form synapses that are in contact with the primary afferent nerve fibers. These pre-synaptic cells comprise about 15% of the taste bud and have been able to be identified by their expression of SNAP-25, a neuronal synapse protein. The Type III cells are believed to transduce sour taste signals and release serotonin upon stimulation from these signals (Richter et al. 2003; Kinnamon et al. 2005; Huang et al. 2006; Clapp et al. 2006; DeFazio et al. 2006; Roper 2006, Huang et al. 2008).

The fourth and final taste cell, Type IV, has not yet been shown to have a true role as a taste receptor. Instead, this small subset of cells located at the base of the taste bud has been tagged as a potential precursor that can give rise to the previously mentioned mature and

functional taste cells. This conclusion was made after pulse-chase studies showed that the basal cells were the first to be marked as cells entered the taste bud (Delay et al. 1986).

The generation of taste bud cells is a complex and not completely understood process. As seen in a typical epidermis, it is generally accepted that a small number of taste bud stem cells divide to give rise to progenitor or transient amplifying (TA) cells. These TA cells will either enter the taste bud as postmitotic, immature taste cells or will divide once again (Miura and Barlow, 2010). While they are known to arise from the local epithelium during development (Barlow and Northcutt, 1995; Stone et al. 1995), little is known regarding the location of these stem and progenitor cell populations that provide this continuous replenishment of cells. Recent research has led to two varying hypotheses. Earlier birthdating studies propose that the functional taste cells come from intragemmal (within the taste bud) basal cells (Delay et al. 1986; Miura et al. 2006). Sullivan's group most recently came to a similar conclusion using label-retaining techniques to identify slow- (potential stem cells) and fast-cycling (mitotically active) cells at peak moments in the circadian rhythm of cell proliferation. They conclude that both stem and progenitor cells are housed within the taste bud in adult mice (Sullivan et al. 2010). In contrast, some studies have indicated that the taste cell generating population of cells lies strictly outside the zone of the taste bud, primarily in the extragemmal or edge cells (Farbman 1980). Okubo's lab provided evidence that many of the functional taste cells in adult mouse taste buds are progeny of cytokeratin 14-expressing progenitor cells (K14). Their cell lineage analysis demonstrated that these K14 descendants derived from cells located outside the taste bud (Okubo et al. 2009). While the dispute concerning taste bud-supplying stem and progenitor cell location continues, it is important to note that it has been shown that multiple progenitors contribute to the cell population in a single bud (Stone et al. 2002). Therefore, both ideas regarding inner and

outer progenitor and stem cell location may in fact be accurate. This possibility of a dual taste cell supply sites warrants further investigation into the origins of cells assisting in the lifelong maintenance of taste buds.

While identifying expression traits that differentiate between stem cells and progenitor cells in the taste system has been troublesome, cell lineage analyses with a few markers have been undertaken. Most recently the role of embryonic Sonic Hedgehog (Shh)-expressing cells as taste bud progenitors was investigated (Thirumangalathu et al. 2009). While it was found that Shh cells gave rise to Types I, II, IV, and perigemmal cells (outside the taste bud) at the early postnatal stage, these same cells were shown to stop expressing Shh after a certain point and can no longer be identified in older adults. Therefore, these Shh-descendent cells may play a role in the initial development of taste buds and the surrounding epithelium but do not act as long-term progenitors to taste cell renewal and maintenance.

However, an earlier study identifies a marker found strictly in basal epithelial cells as a common progenitor that gives rise to Type II and III cells, indicating a possible common lineage. This previously mentioned marker, cytokeratin-14 (K14), was initially found to be expressed in the immature cells of taste buds (Asano-Miyoshi et al. 2008). More extensive lineage tracing studies have shown that the K14 expressing cells outside the taste bud function as bipotential progenitor cells in that they give rise to both functional taste cells and taste bud-surrounding keratinocytes (Okubo et al. 2009). These investigators go on to identify a progenitor cell pool by noting that the K14-expressing cells outside the taste bud also express cytokeratin-5 (K5), Trp63, and Sox2.

With $K14^{+}Trp63^{+}K5^{+}Sox2^{+}$ cells identified as a potential progenitor pool, the questions of what progeny are produced, their patterns of division, and how this pertains to differentiation

into functional taste cells remain. In addition to attributes of the progenitor pool, the mechanism regulating the progenitor cells differentiating activity is still uncertain. Previous research shows that the maintenance of the taste bud is a highly coordinated process between the production of taste cells via the cell cycle and the concurrent apoptotic events removing cells from the taste bud (Takeda et al. 1996; Takeda et al. 2000; Huang et al. 2001; Ueda et al. 2008). The timing mechanism involved in the homeostatic nature of the taste bud has only recently been investigated. This approach was taken from the perspective of understanding the role of a type of regulatory protein found in the cell cycle, cyclin-dependent kinase inhibitors (CDKI). In general, progression through the cell cycle is regulated by cyclin-dependent kinase (CDK) activity. The aforementioned CDKIs have the capability to negatively control CDK activity, hence, halting cell cycle progression. The search into CDKI activity in taste cells led to the report of one CDKI (p27^{Kip1}) being expressed in mature taste buds (Hirota et al. 2001). While Hirota's work looked exclusively at the Cip/Kip family of cell cycle regulators, recent studies have indicated that the other major group of CDKIs, the INK4 family, is also expressed *in vitro* in the taste epithelium (Nakamura et al. 2010). Although studies into both CDKIs are thus far limited, we have chosen to focus on p27^{Kip1}. Our previous studies with p27^{Kip1}-null mice marked by BrdU pulse-labeling show an increase in the number of cells entering the taste bud as well as increased turnover. However, a closer look reveals that taste bud size appeared to be unaltered (Harrison et al. manuscript under review). This warrants further investigation into not only p27^{Kip1}'s role as a timing mechanism of cell entry and exit from the taste bud but also its apparent role in the regulation of taste cell number.

An increased understanding of factors regulating taste cell production and the environment from which mature taste cells originate can provide pivotal information as to how

the fates of taste cells are determined as they progress through the taste bud into functional taste cell types. Fate mapping studies thus far have answered few questions regarding cell lineage and how cells obtain their specificity as a transducer of taste signals. This is primarily due to these studies having asked questions at the population level. Seeing as the existing techniques mark large populations of cells, they are unable to provide the cell-level resolution required to study individual progenitor cell potency. Nonetheless, from these investigations a few hypotheses have been developed regarding taste cell lineage from its earliest time point prior to differentiation at the stem/progenitor cell level to the point where it acts as a reliable source of taste transduction. Conclusions from previous mosaic analysis studies have shown that multiple progenitors contribute to the overall maintenance of the taste bud. However, it is not known whether all of the identified progenitor cells contribute equally to the taste bud (Stone et al. 2002). This, in conjunction with progenitor cells that appear to exclusively supply the taste bud, indicates that the taste cell lineages may be distinct from one another. These authors go on to hypothesize the possible lineage pathways mature taste cells follow and address them with regards to the restriction of the progenitor cells. The first possibility is the stricter of the two in that one embryonic progenitor will ultimately give rise solely to a basal cell that will produce only one type of differentiated taste cell. On the other hand, it is possible for the embryonic progenitor line to give rise to a multipotent stem cell that will in turn produce the aforementioned lineage-restricted basal cells (Stone et al. 2002). Another possible lineage pathway that has been developed illustrates the possibility of progenitor cells having varying levels of potency (Miura et al. 2006). This conclusion came about after protein expression studies indicated that both Type II and Type III taste cells express Mash1, a protein expressed during central and peripheral nervous system development (Lo et al. 1991; Guillemot et al. 1993). These findings provide

evidence in favor of a common lineage pathway being shared by Type II and Type III taste cells, entirely separate from that of Type I cells. Figure 1 illustrates these three potential cell lineage pathways.

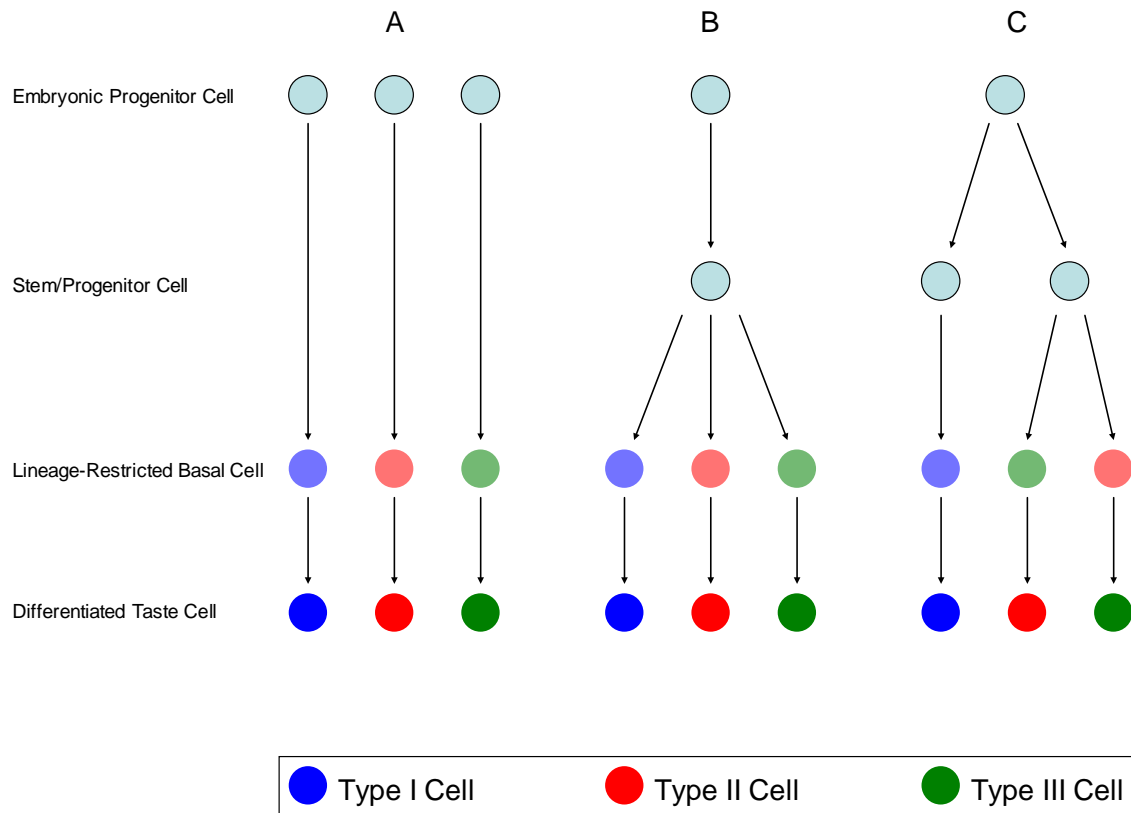


Figure 1. Possible cell lineage pathways of mature taste cells. Diagrams A and B contrast the pathways derived from unipotent as opposed to multipotent progenitors, respectively. In the former generation of clones will always result in one taste cell type per progenitor cell. In the latter the progenitor cell is able to give rise to any of the three functional taste cell types. Diagram C illustrates the proposal from more recent studies in cell lineage where progenitors may display the capability to have varying levels of potency.

In an effort to obtain a better understanding of the mechanism behind taste cell renewal, we first set out an experiment to better understand the expression patterns and influence that the CDKI p27^{Kip1} has on the functional classes of taste cells in the bud given the increase in cellular proliferation we have seen when the gene is removed. Our previous approaches have noted definite p27^{Kip1} expression in Type II cells and probable expression in Type III cells seen in tissue sections. Co-expression with Type I cells was inconclusive. The lab also tried to determine whether loss of p27^{Kip1} influences the proportions of taste cell types in the bud. However, the morphology of the Type I and most Type III cells in tissue sections has made their analysis more difficult. To overcome this we have isolated the circumvallate papillae (CVP) and enzymatically broken up the endorgans it contains to produce a population of dispersed cells. This allows for all taste cell types to be visualized as a single layer of cells without restrictions from neighboring tissues or a loss of cellular processes previously seen in tissue sections.

In conjunction with our investigation into p27^{Kip1}, we designed a series of experiments to study progenitor cell potency using a new technique called Mosaic Analysis with Double Markers (MADM). Unlike previous approaches that have provided data from a mass population of labeled cells, the MADM approach is able to give simultaneous labeling and gene knockout in clones of mitotically active cells at a single cell resolution level via Cre-mediated interchromosomal recombination (Zong et al. 2005). We have applied the MADM scheme to the aforementioned K14 expressing cells due to their previously noted role as a progenitor candidate to taste cell renewal (Asano-Miyoshi et al. 2008; Okubo et al. 2009). These experiments will allow for us to determine the true potency of K14 expressing cells as well as the symmetry of the progenitor cell divisions either into or in the surrounding tissues of the taste bud. Ultimately, we plan to take advantage of the ability of the MADM technique to provide a mosaic analysis at the

single cell level by arranging the schematic around a knockout of the p27^{Kip1} allele. This will allow for us to solidify whether or not the role that p27^{Kip1} has in taste cell turnover expands beyond that of its CDKI activity.

CHAPTER 2

FUNCTIONAL EXPRESSION OF THE CYCLIN-DEPENDENT KINASE INHIBITOR p27^{Kip1} IN TASTE CELLS

Preston D. Moore^{1,2}, Theresa A. Harrison¹, Jarrod D. Sword¹ and Dennis M. Defoe¹

¹Department of Anatomy and Cell Biology, James H. Quillen College of Medicine, East Tennessee State University, Johnson City, TN 37614

²Biomedical Science Graduate Program, James H. Quillen College of Medicine, East Tennessee State University, Johnson City, TN 37614

Address for correspondence:

Theresa A. Harrison, Ph.D.
Department of Anatomy and Cell Biology
James H. Quillen College of Medicine
East Tennessee State University
PO Box 70582
Johnson City, TN 37614-1708
Phone: (423) 439-2122
FAX: (423) 439-2017
Email harrisot@etsu.edu

ABSTRACT

Mammalian taste buds contain several specialized cell types that transduce taste signals via the primary afferent nerves. While it is understood that these cells undergo continuous turnover, little is known regarding how the population of cells in a taste bud are produced and retained. The cyclin-dependent kinase inhibitor p27^{Kip1} has been shown to influence cell number in several developing tissues, by coordinating cell cycle exit during cell differentiation. Previous studies into taste cell turnover have confirmed expression of p27^{Kip1} in the taste bud. However, the expression pattern of p27^{Kip1} throughout the bud as well as the role it may have in the regulation of taste cell number has yet to be examined thoroughly. Here, we implement a new approach to investigate these issues by examining p27^{Kip1} knockout adult mice.

INTRODUCTION

As mentioned previously, taste cells have a limited lifespan and must undergo continuous turnover throughout the taste bud, a process taking approximately 10-14 days (Farbman 1980). What appears to keep the taste bud a functional endorgan is the ability for taste cells to maintain not only proper cell-cell and cell-afferent nerve interactions but also viable populations of subtype variety while taste cell turnover is continuing (Chaudhari and Roper, 2010). The mechanism that regulates constant cellular renewal in the taste bud is not well understood. Nonetheless, some features about this system can be hypothesized based upon other mechanisms of cell proliferation and differentiation seen elsewhere. Therefore, an approach to better understanding taste cell turnover is to investigate the role that cell cycle proteins may have in the taste bud.

In general, the cell cycle is managed by the balanced expression of both positive and negative signals. The positive signals, known as cyclin-dependent kinases (CDK), play a role in the progression of cellular growth via the complexes they form with the cyclin protein (Pines 1993; Sherr and Roberts, 1999). Just as important as progression through the cell cycle is its inhibition, as uncontrolled proliferation of cells through the cell cycle can ultimately lead to tumor development. The negative cell cycle control proteins, appropriately called cyclin-dependent kinase inhibitors (CDKI), act by preventing CDK activity after the formation of its complex with the appropriate cyclin; hence, preventing progression of the cell cycle (Sherr and Roberts, 1999). There are two primary classes of CDKIs that have been identified, Cip/Kip and INK4. The Cip/Kip family includes p21^{Cip1}, p21^{waf1/Cip1/Sd1/ndm-6}, p27^{Kip1}, and p57^{Kip2} (Sherr 1995). The INK4 family consists of p15^{INK4b}, p16^{INK4a}, p18^{INK4c}, and p19^{INK4d} (Drexler 1998).

Up until just recently, only one of the CDKIs has been shown to be expressed within the taste buds, p27^{Kip1} (Hirota et al, 2001). However, the latest studies show that members of the INK4 family are expressed as well in the taste epithelium *in vitro* (Nakamura et al. 2010).

While expression of both families of CDKIs has been found in the taste epithelium, their putative activity in regulating taste cell turnover remains to be determined. In the Cip/Kip family, p27^{Kip1} has been shown to play a pivotal role as a timer to cell cycle exit in the precursor cells of developing sensory systems (Durand et al. 1998; Durand and Raff, 2000). In various organ systems knockout analysis of p27^{Kip1} displayed an overall increase in size as well as the number of cells, often leading to tumor development (Sherr and Roberts, 1999). Previous studies in our lab using p27^{Kip1}-null mice have shown that despite an increased rate of cellular turnover and apoptotic events, evidenced by increased BrdU labeling, and a minimal increase in tongue size, the number and size of the taste buds remains unchanged (Harrison et al, manuscript under review). This raises the question of how the individual taste cells are affected despite the increase in turnover. More specifically, are the relative proportions of taste cell subtypes between wild-type and mutant (p27^{Kip1}-null) mice altered due to this noted increase in cell proliferation? Our previous attempts to answer this question looked at taste cell counts from tissue sections of CVP tissue. One minor setback of using frozen sections to look at the effect p27^{Kip1} has on taste cell number is that there tends to be a bit of discrepancy when evaluating labeling of taste cells that appear to be separated between sections. Also, as opposed to the cytoplasmic marker (Myoshi et al, 2001) used to identify Type II cells (PLC β -2), the markers for Type I (NTPDase2) and Type III (SNAP-25) are located at the plasma membrane (Bartel et al, 2006) and synapses (Yang et al, 2000), respectively. These marker restrictions have made identifying positively labeled Type I or Type III cells *in situ* difficult.

To overcome these barriers we have taken a different approach to analyzing labeled taste cells. In the following experiment dispersed cell preparations of taste buds enzymatically dissociated from the CVP of wild-type and $p27^{Kip1}$ knockout mice were made and labeled with the previously mentioned taste cell marker antibodies. These preparations will minimize the problems in counting labeled cells in tissue section by providing a single cell layer for visualization, while also enabling whole cell labeling.

MATERIALS AND METHODS

Mice and Genotyping

Hemizygous $p27^{Kip1}$ mice (+/-), on a C57BL/6 background, were purchased from The Jackson Laboratory (Bar Harbor, ME) and used to set up a breeding colony. Animals were housed in the Animal Care Facilities at ETSU College of Medicine in accordance with Association of Assessment and Accreditation of Laboratory Animal Care (AAALAC) guidelines. Tail snips were taken from all mice at or before 4 weeks of age and genomic DNA was extracted and purified using an Extract-N-Amp Tissue PCR Kit (Sigma-Aldrich, St. Louis, MO). Genotypes were determined by performing PCR amplification of the wild-type and mutant $p27^{Kip1}$ alleles. One common sense primer (5'-TGG AAC CCT GTG CCA TCT CTA T-3') was used to detect both alleles, while the antisense primers employed were specific for the wild-type allele (5'-GAG CAG ACG CCC AAG AAG C-3') and the *neo*-disrupted allele (5'-CCT TCT ATG GCC TTC TTG ACG-3'). PCR was performed for 40 cycles with an annealing temperature of 55 °C. Oligonucleotide products were then resolved on a 2% agarose gel and visualized after staining with 0.01% Sybr Gold (Invitrogen, Carlsbad, CA). The wild-type allele resulted in amplification of a 1300-bp product and the null allele a 600-bp product.

Preparation of Circumvallate Papillae Cleft Cell Dispersions

Mice were euthanized by CO₂ asphyxiation and whole tongue tissues were surgically removed. Following extraction, tongue tissue was injected with 1% Dispase dissolved in antibiotic treated Basic Salt Solution (BSS), similar to previous studies (Ozdener et al. 2006). Injections were made parallel to and just beneath the epidermis with the needle being inserted at the cut edge of the tongue, the posterior end. The needle was carefully advanced to the anterior end of the tissue, avoiding contact with the CVP, and slowly retracted to the posterior end of the tissue as Dispase was being injected. Injected tissue was allowed to incubate for 15 minutes at room temperature in BSS. Following incubation, the epidermal layer was stripped from the rest of the tongue. In doing so, the two invaginations of the CVP that contain the taste buds were also removed. Clefts were trimmed away from the surrounding superfluous tissue and submitted to two brief (5-10 seconds) washes in Isolation Buffer Solution (IBS) consisting of 0.5mM EGTA, 0.4μM EDTA, 1% polyvinylpyrrolidone, 0.15M NaCl, 15mM HEPES buffer (Luo et al. 2009). Tissue was then transferred into a microcentrifuge tube containing 100μL solution of 0.05% Trypsin in IBS pre-heated to 37°C and placed in 37°C oven for 10 minutes. Trypsin was then inactivated with 20μL of 1% Trypsin Inhibitor in IBS. Following inactivation, the protease-treated tissue was triturated with a 200μL pipette set at 40μL to dissociate the tissue into single cells and cell clusters. Cell-Tak (BD Biosciences, Bedford, MA) coated slides were used for mounting of cell suspension and prepared the day of taste cell isolation following the manufacturer protocol for adsorption to slides. Prior to centrifugation, 11.8μL of Cell-Tak (2.1 mg/mL in 5% acetic acid) was applied onto the slide and allowed to evaporate. The slides were then rinsed with distilled water and dried at room temperature. Suspensions of dispersed cells were centrifuged onto Cell-Tak coated slides via the Shandon-Elliot Cytospin (SCA-0030,

Shandon Southern Instruments, Surrey, England) at 2000 rpm for 3 minutes. Slide-mounted cells were then submitted to a 10 minute fixation period with 4% PFA followed by two 10-minute washes with PBS. Dispersed cell preparations were stored at -20°C until use for immunohistochemistry (IHC).

Cell Dispersion Triple-Labeling Immunohistochemistry

Tongue tissue containing the CVP was surgically removed and processed for CVP cleft cell dispersion as previously described. Preparations were first incubated in 10% normal serum in standard incubation buffer (0.5% Bovine Serum Albumin and 0.4% Triton-X-100 in 0.1M PBS), followed by overnight incubation with a combination of primary antibodies for PLC β -2 (1:1000; Santa Cruz Biotechnology, Inc., Santa Cruz, CA) and SNAP-25 (1:500; Chemicon, Temecula, CA) with rinsing occurring between each incubation period. Primary antibody labeling for PLC β -2 was identified by biotinylated secondary antibody (1:400; Jackson ImmunoResearch Laboratories, West Grove, PA) at room temperature for 2 hours and streptavidin-conjugated Alexa Fluor 488 (1:600) for 1 hour. Primary antibody labeling for SNAP-25 (1:500; Chemicon, Temecula, CA) was seen with a secondary IgG directly conjugated to Alexa Fluor 647. After rinsing, sections were again blocked in normal serum then incubated overnight in primary antibody specific for NTPDase2 (1:1000; Dr. Jean Sevigny, CHUQ, Quebec, Canada). Visualization of NTPDase2 labeled cells was confirmed with a species-specific secondary antibody conjugated to Alexa Fluor 555.

Cell Dispersion p27^{Kip1} Co-Expression Immunohistochemistry

Tongue tissue containing the CVP was surgically removed and processed for CVP cleft cell dispersion as previously explained. The dispersed cells first underwent antigen retrieval by immersion in 10 mM citrate buffer (pH 6.0, 15 min, 97°C) and were then incubated in 10% normal serum in standard incubation buffer, followed by overnight incubation at 4°C with mouse monoclonal anti-p27^{Kip1} (1:100; Transduction Laboratories, Lexington, KY). All subsequent reagents were also diluted in incubation buffer. Primary antibody labeling was detected by sequential application of biotinylated secondary antibody (1:400; Jackson ImmunoResearch Laboratories, West Grove, PA) at room temperature for 2 hours and streptavidin-conjugated Alexa Fluor 488 (1:600) for 1 hour. After rinsing, sections were again blocked in normal serum and incubated in primary antibody specific for either PLCβ-2 (1:1000), NTPDase2 (1:1000), or SNAP-25 (1:500) and labeling was visualized with an IgG against the appropriate species, conjugated to Alexa Fluor 555 (1:400).

Confocal Microscopy and Data Analysis

Specimens prepared for immunofluorescence microscopy were viewed in a Leica SP confocal laser scanning microscope (Leica, Heidelberg, Germany) equipped with an inverted fluorescence microscope and a 20X infinity-corrected objective. A series of optical sections was obtained at 1μm steps thorough the z-axis of the dispersed cells. Series images were used to construct an extended focus image consisting of all optical sections in the data set (i.e., a maximum projection). For the area containing the dispersed cells, a total of six fields of view were analyzed to obtain cell counts. The first field was selected at random, with this point of origin remaining the same for all cell dispersion preparations analyzed. The remaining five areas

of analysis were determined by a systematic pattern of shifting two complete fields of view to the right and one complete field of view down, carrying back over to the leftmost border of the dispersed cell preparation when the right-side boundaries were met and being careful not to overlap into fields of view already counted. All cells within a specific area that were labeled by each of the antibodies were counted and expressed as a percentage of the total number of labeled cells. The results were then evaluated by Chi-square analysis using the MatLab statistical software package.

RESULTS

Previous experiments looking into p27^{Kip1} co-labeling in tissue sections of the CVP were able to show definitive co-labeling with p27^{Kip1} with PLCβ2 in Type II cells (Harrison et al, manuscript under review). For the two remaining cell types, Type III cells could be identified as also expressing p27^{Kip1} occasionally, but the relative congestion and orientation of taste cells inside the taste bud along with the location of the antigens used as markers for Type I and Type III cells made co-labeling studies with p27^{Kip1} in tissue sections inconclusive. In order to get around this dilemma, dispersed cell preparations were made from enzymatically treated CVP tissue. These preparations allow for all cells of the CVP to be visualized as a single-celled layer; and therefore, diminish the confusion in determining cell boundaries previously encountered when cells were labeled in whole sections.

After dispersed cell preparations were made, it was important to ensure two things before progressing with p27^{Kip1} co-labeling studies. First, we needed to make sure that labeling for all three taste cell types was possible after tissue treatment with the aforementioned trypsin/trituration technique. Figure 2 illustrates a complete, triple-labeled dispersed cell

preparation for both wild-type and mutant animals. After IHC, most preparations contained many small, circular, unlabeled cell clusters. These are most likely keratinocytes, small cells that make up the surrounding lingual epithelium. In addition to the keratinocytes, positive labeling for all taste cell types was seen in individual cells as well as larger clusters of cells. Type I cells, labeled with anti-NTPDase2 (red), appear most prevalent in dispersed cell preparations. Type II cells, identified by anti-PLC β 2 (green), and Type III cells, marked with anti-SNAP25 (magenta), were fewer in number but successfully labeled as well.

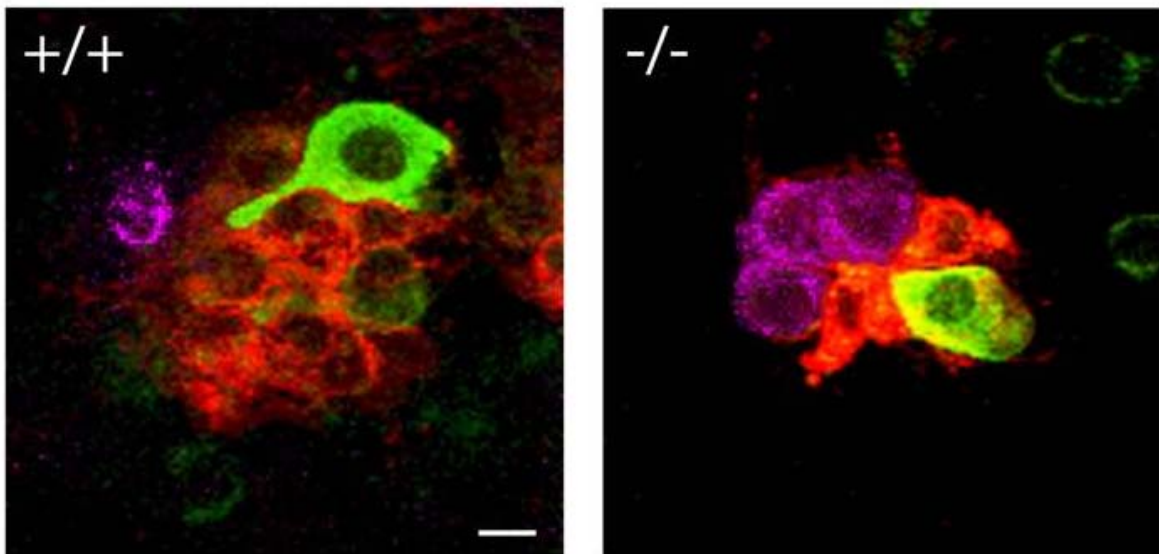


Figure 2. Triple-labeled cell clusters from dispersed cell preparations. Maximum projection confocal images of both wild-type (left) and p27^{Kip1} knockout mice demonstrate sufficient immunohistochemical labeling for all three taste cell types. In both genotypes, Type I cells (anti-NTPDase2; red) appear most prevalent, but labeling for Type II (anti-PLC β 2; green) and Type III (anti-SNAP25; magenta) is also noted in single cells as well as cell clusters. Isolated and clusters of unlabeled cells, keratinocytes, were also seen in the dispersed cell preparations (Scale bar = 10 μ m.).

Secondly, in order to verify reproducibility of the dispersion technique, immunolabeled cell types needed to be quantified to confirm there was little variation from animal to animal in wild-type mice before we could investigate p27^{Kip1} gene expression on taste cell number. With minimal variation detected (data not shown), we proceeded with cell dispersion preparation analyses of the taste cell subtype population proportions between wild-type and p27^{Kip1}-null mice. Average cell counts for each taste cell type expressed as a percentage of the whole labeled cell population are seen in figure 3. Our data indicate that no significant difference was detected between wild-type and mutant mice in the relative number of taste cells identified by the triple-labeled cell dispersion preparations. Furthermore, this demonstrates that the dispersed cell preparation should be an adequate approach for fully analyzing the colabeling of individual taste cell types with p27^{Kip1}.

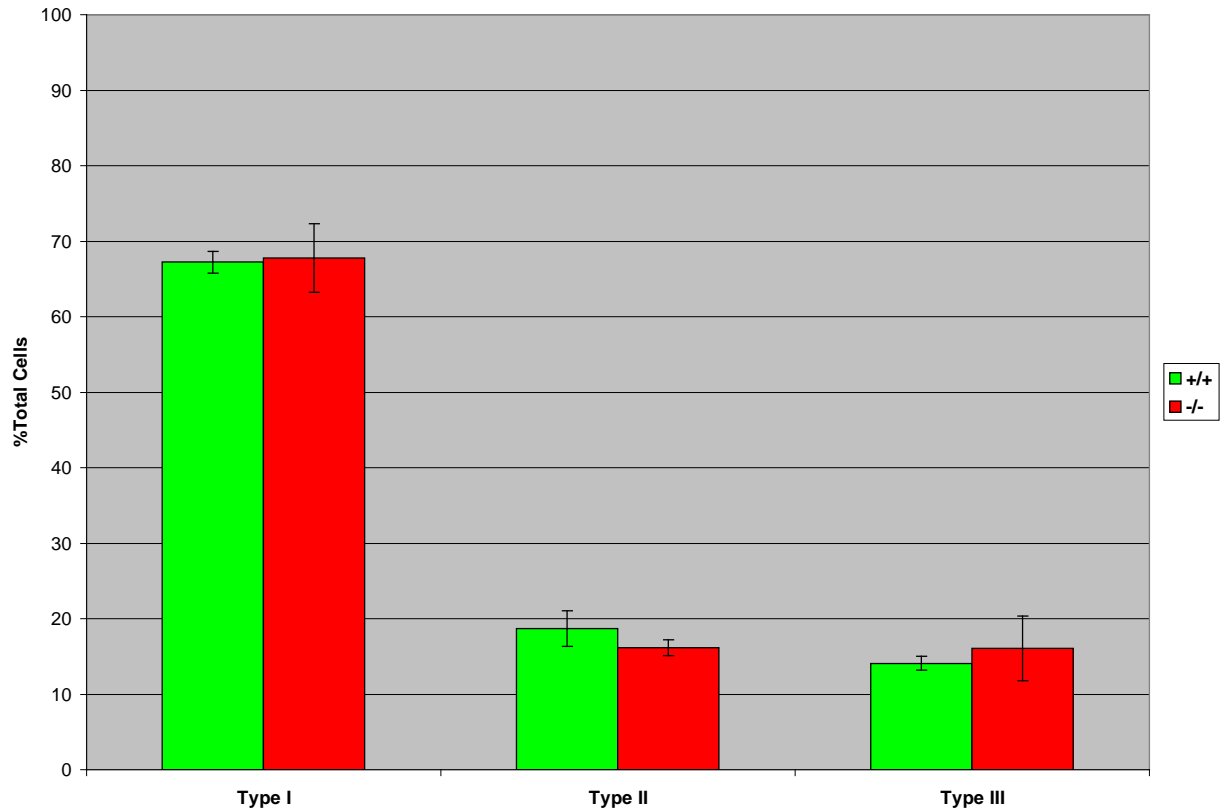


Figure 3. Loss of p27^{Kip1} function does not alter relative taste cell subtype populations. Quantification of functional taste cell types expressed as a relative percentage of total labeled dispersed cells (Mean \pm SEM; n=3) for each genotype (Wild-type, green; Mutant, red). Chi-square analysis indicates no significant difference between the two genotypes with respect to the distribution of the three taste cell types ($\chi^2 = 2.348$; p = .309).

With confirmation that the technique was reliable, colabeling analysis of p27^{Kip1} expression in different functional taste cell types could be carried out. Dispersed cell preparations were made in the same manner from wild-type mice and processed for double-label IHC of p27^{Kip1} and one of the three taste cell markers as previously described. All preparations were similar in appearance to the triple-labeling study in that single cells and cell clusters were noted throughout the slide. In order to see sufficient p27^{Kip1} labeling, antigen retrieval had to be

performed on cell dispersion preparation slides. The antigen retrieval did not appear to have any effect on the antigenicity of the taste cells to our antibody markers or the adhesion of single cells and cell clusters to the slides. Following IHC, keratinocytes were noted in similar fashion to the previous cell dispersion experiment. Figure 4 confirms what has been seen in whole sections thus far: p27^{Kip1} is co-expressed in conjunction with Type II cells. However, the cell dispersion preparations clarified co-labeling analyses for the other two cell types. Type III cells showed questionable co-labeling in whole sections, but when the cells were dispersed, co-labeling of Type III cells and p27^{Kip1} was noted on several occasions. It is important to note that not all Type II and Type III cells express p27^{Kip1}. Type I cells, on the other hand, still did not show any expression of p27^{Kip1} in the dispersed cell preparations. This confirms the results of analysis of whole CVP sections as well.

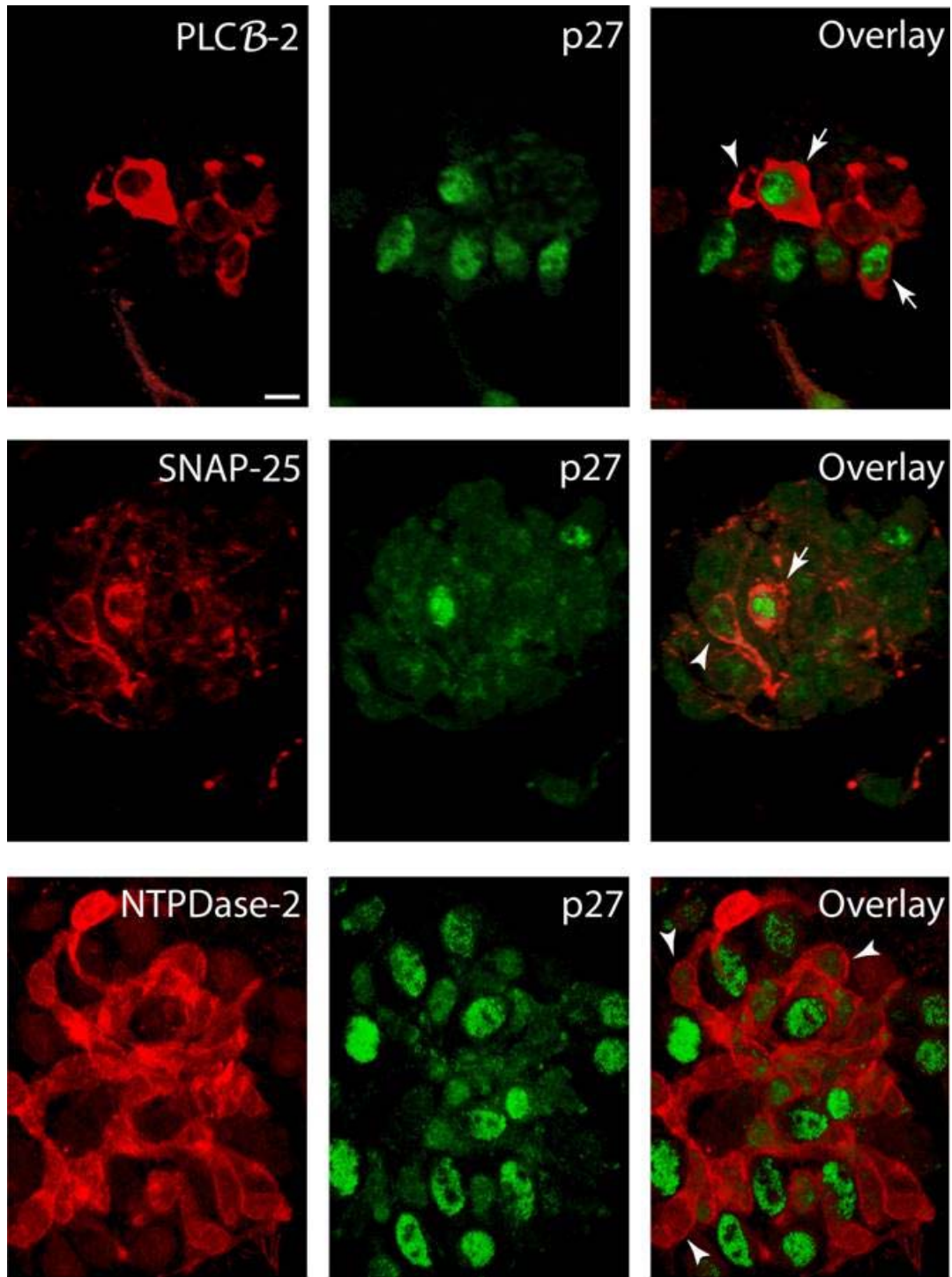


Figure 4. Co-Expression of $p27^{Kip1}$ (green) and individual taste cell type markers (red) in wild-type mice. Maximum confocal projection images illustrating type II (PLC β -2) and Type III (SNAP-25) cells that are colabeled with $p27^{Kip1}$ are indicated by arrows, while single-labeled cells are marked by arrowheads. Type I (NTPDase-2) cells bodies are negative for $p27^{Kip1}$ immunoreactivity (arrowheads). Scale bar = 10 μ m.

DISCUSSION

In the present study we provide evaluation of a new methodology for understanding the underlying mechanisms of taste cell number and replacement. Our previous studies into gene function that may regulate cell cycle exit and differentiation into the taste bud as it relates to taste cell number had limitations. We were able to note through BrdU labeling that the taste cells displayed an increased rate of proliferation when the CDKI that we investigated, p27^{Kip1}, was knocked out. Given this, one would expect an increase in the turnover of taste cells might suggest changes in the taste cell populations. Furthermore, because loss of p27^{Kip1} function has been noted in other organ systems to result in an increase in cell number and organ size, it was critical to see if p27^{Kip1} played a role in not just the number of taste cells within a taste bud but also the ratio of functional taste cell types in relationship to one another. However, before we could verify this, we had to determine if p27^{Kip1} was expressed in all three functional taste cell types, a question never before investigated. Our laboratory's previous work illustrates expression of p27^{Kip1} in Types II and III cells in intact taste buds. Now, using the enzymatically dispersed cell preparation, we can confirm that p27^{Kip1} is expressed in these two taste transducing cell types but not the Type I cells. In turn these dispersed cell preparations later revealed that the overall distribution of expression of proteins specific for different functional types of taste cells did not appear to change between wild-type and mutant (p27^{Kip1}-null) animals. Therefore, even though we notice this selectivity of p27^{Kip1} expression, the loss of gene function does not appear to disrupt the relative populations of taste cell subtypes. In conjunction with our laboratory's previous data regarding enhanced cell proliferation upon gene knockout, it does not appear that p27^{Kip1} has a role in taste cell differentiation in spite of the participation of the protein in regulating cell cycle entry and exit. However, this needs to be investigated further.

REFERENCES

- Bartel DL, Sullivan SL, Lavoie EG, Sevigny J, Finger TE. Nucleoside triphosphate diphosphohydrolase-2 is the ecto-ATPase of type I cells in taste buds. *J. Comp. Neurol.* 2006; 497: 1-12.
- Chaudhari N, Roper S. The cell biology of taste: Cells, synapses, and signals in taste buds. *The Journal of Cell Biology.* 2010; 3: 285-296.
- Drexler HG. Review of alterations of the cyclin-dependent kinase – inhibitor INK4 family gene p15, p16, p18, and p19 in human leukemia-lymphoma cells. *Leukemia.* 1998; 12: 845-859.
- Durand B, Fero ML, Roberts JM, Raff MC. p27^{Kip1} alters the response of cells to mitogen and is part of a cell intrinsic timer that arrests cell cycles and initiates differentiation. *Curr. Biol.* 1998; 8: 431-440.
- Durand B, Raff M. A cell-intrinsic timer that operates during oligodendrocyte development. *Bioessays.* 2000; 22(1): 64-71.
- Farbman AI. Renewal of taste bud cells in rat circumvallate papillae. *Cell Tissue Kinet.* 1980; 13: 349-357.
- Harrison TA, Adams LBS, Moore PD, Perna MK, Sword JD, Defoe DM. Accelerated turnover of taste bud cells in mice deficient for the cyclin-dependent kinase inhibitor p27^{Kip1}. *BMC Neurosci.* (submitted).
- Hirota M, Ito T, Okudela K, Kawabe R, Hayashi H, Yazawa T, Fujita K, Kitamura H. Expression of cyclin-dependent kinase inhibitors in taste buds of mouse and hamster. *Tissue & Cell.* 2001; 33: 25-32.
- Luo X, Okubo T, Randell S, Hogan BL. Culture of endodermal stem/progenitor cells of the mouse tongue. *In Vitro Cell Dev Biol Anim.* 2009; 45(1-2): 44-54.
- Miyoshi MA, Abe K, Emori Y. IP(3) receptor type 3 and PLCbeta2 are co-expressed with taste receptors T1R and T2R in rat taste bud cells. *Chem. Senses.* 2001; 26: 259-265
- Nakamura S, Kamakura T, Ookura T. Tongue epithelial KT-1 cell-cycle arrest by TGF-beta associated with induction of p21(Cip1) and p15 (Ink4b). *Cytotechnology.* 2009; 61(3): 109-16.
- Ozdener H, Yee KK, Cao J, Brand JG, Teeter JH, Rawson NE. Characterization and Long-Term Maintenance of Rat Taste Cells in Culture. *Chem. Senses.* 2006; 31: 279-290.

Pines J. Cyclins and cyclin-dependent kinases: take your partners. *Trends Biochem. Sci.* 1993; 18: 195-197.

Sherr CJ. D-type cyclins. *Trends Biochem Sci.* 1995; 20(5): 187-90.

Sherr CJ, Roberts JM. CDK inhibitors: positive and negative regulators of G₁-phase progression. *Genes & Development.* 1999; 13: 1501-1512.

Yang R, Crowley HH, Rock ME, Kinnamon JC. Taste cells with synapses in rat circumvallate papillae display SNAP-25-like immunoreactivity. *J. Comp. Neurol.* 2000; 424: 205-215.

CHAPTER 3

MOSAIC ANALYSIS WITH DOUBLE MARKERS IDENTIFIES TASTE CELL PROGENY IN ADULT MICE

Preston D. Moore^{1,2}, Theresa A. Harrison¹, Jarrod D. Sword¹ and Dennis M. Defoe¹

¹Department of Anatomy and Cell Biology, James H. Quillen College of Medicine, East Tennessee State University, Johnson City, TN 37614

²Biomedical Science Graduate Program, James H. Quillen College of Medicine, East Tennessee State University, Johnson City, TN 37614

Address for correspondence:

Theresa A. Harrison, Ph.D.
Department of Anatomy and Cell Biology
James H. Quillen College of Medicine
East Tennessee State University
PO Box 70582
Johnson City, TN 37614-1708
Phone: (423) 439-2122
FAX: (423) 439-2017
Email harrisot@etsu.edu

ABSTRACT

The differentiation pathway(s) from epithelial progenitor cells to functional subtypes of cells in mammalian taste buds operate not only during development but also throughout life as taste cells are continuously replaced. These pathways, however, are not yet clearly understood. In the present study, we have applied a new fate mapping technique to trace taste cell renewal at single-cell resolution in normal mouse circumvallate papillae. This new technique, Mosaic Analysis with Double Markers (MADM), uses rare, Cre-mediated *interchromosomal* recombination events during mitosis to reconstitute functional GFP and RFP genes, with one of the proteins expressed in each daughter cell and its subsequent progeny. Successful MADM events will allow for a better understanding of the progenitor cell potency that supplies cells to adult mouse taste buds.

INTRODUCTION

While previous studies have shown bipotential progenitor properties of K14 expressing cells surrounding the taste bud, a clear answer as to which taste cell types are derived from these cells remains to be determined. These same cells have also been marked for expression of cytokeratin-5 (K5), Trp63, and Sox2 (Okubo et al. 2009). However, for the focus of this study we are looking exclusively at K14 potency to the taste bud. Lineage tracing of cells from this potential progenitor pool will provide a direction for future investigations in the signaling pathways for taste cell turnover and cell differentiation. Earlier lineage tracing studies of taste cells, while providing pivotal information regarding the expression characteristics of the aforementioned progenitor pool, have resulted in the marking of large populations of cells. This makes studying the potency of single progenitor cell lines seemingly impossible. To resolve this conflict we have implemented a new technique that will allow for similar lineage tracing experiments to be completed at a single cell level, which is necessary to completing a true clonal analysis. In conjunction with lineage tracing this technique will provide mosaicism on two levels, phenotype and genotype between labeled cells, described in further detail later, as well as answer questions regarding the cell division symmetry of progenitor cells. This new technique is called Mosaic Analysis with Double Markers (MADM).

Zong and his colleagues developed the MADM strategy as a way to more effectively study gene function as it relates to tracking single cells and subsequent progeny throughout development (Zong et al. 2005). MADM uses the Cre-LoxP system to obtain rare, *interchromosomal* recombination events that ultimately provide labeled cells homozygous for either the wild-type or mutant genotype across a heterozygous background. Furthermore, it

allows for synchronized labeling and gene knockout in clones of somatic cells (Zong et al. 2005, Muzumdar et al. 2007). This new technique provides many advantages over previous mosaic analysis techniques previously used. First, the efficiency of cell labeling can be adjusted depending on the Cre-line used. In the Cre/LoxP recombination system, Cre, a DNA recombinase enzyme, is able to excise DNA segments flanked by LoxP sites (Sternberg et al. 1981; Stricklett et al. 1999) Zong has applied this system to ultimately produce functional green (GFP) and red fluorescent proteins (RFP) once recombination occurs in the MADM scheme. Moreover, Zong found that success of MADM recombination events is dependent upon the strain of Cre used, as efficiency has been shown to vary anywhere from 0.001% to 5% of the cell population being labeled by MADM (Zong et al. 2005). In each of the various Cre lines studied thus far, the MADM technique has allowed for simultaneous visualization of cells containing the gene knockout, a feature that is difficult to accomplish in the Cre-mediated *intrachromosomal* recombination events used previously. While this technique is currently limited to the ROSA26 locus on chromosome 6, its ability to provide resolution of single cells makes MADM an ideal technique for lineage tracing studies. Figure 5 illustrates the targeting vectors upon which the MADM scheme acts as well as those vectors for our Cre-recombinase strains of interest.

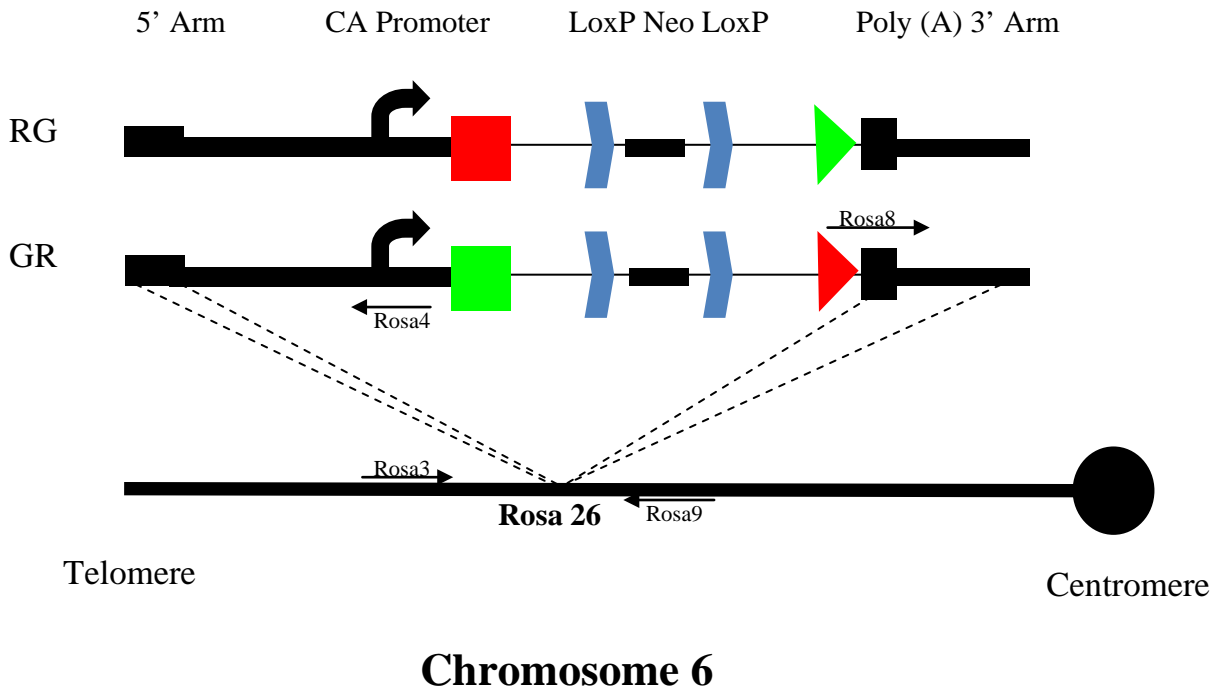


Figure 5. Target vector for MADM knockin mice. The MADM target vector possesses transgenes targeted to the ROSA26 locus on copies of chromosome 6. The RG strain contains the sequence coding for the amino (N) terminus for green fluorescent protein (GFP) and the carboxyl (C) terminus for red fluorescent protein (RFP). The GR strain contains the RFP N-terminus and the GFP C-terminus. The two termini are split by an intron containing the LoxP site on each chromosome. For our experiment, this LoxP site will be targeted by a Cre-recombinase that is either ubiquitously expressed (Hprt-Cre) or tissue-specific (K14-Cre).

The MADM approach to lineage tracing begins with two strains of mice that possess separate transgenes targeted by homologous recombination to the same locus, ROSA26, on both copies of chromosome 6. One strain contains the sequence coding for the amino (N) terminus for green fluorescent protein (GFP) and the carboxyl (C) terminus for red fluorescent protein (RFP), hereon identified as GR. The second strain is the exact opposite, containing the N-terminus for RFP and C-terminus for GFP, identified as RG. The N and C terminal fluorescent protein sequences are split by an intron containing the LoxP site on each chromosome.

Subsequent and patterned breeding of both of these strains with a third strain expressing Cre, a DNA splicing enzyme, results in progeny containing all components of the MADM scheme as noted in the initial step of figure 6. Here, the cells in G_1 display the RG and GR strains in a reciprocally chimeric fashion as well as the Cre-recombinase enzyme that targets the LoxP sites on each chromosome for eventual DNA recombination.

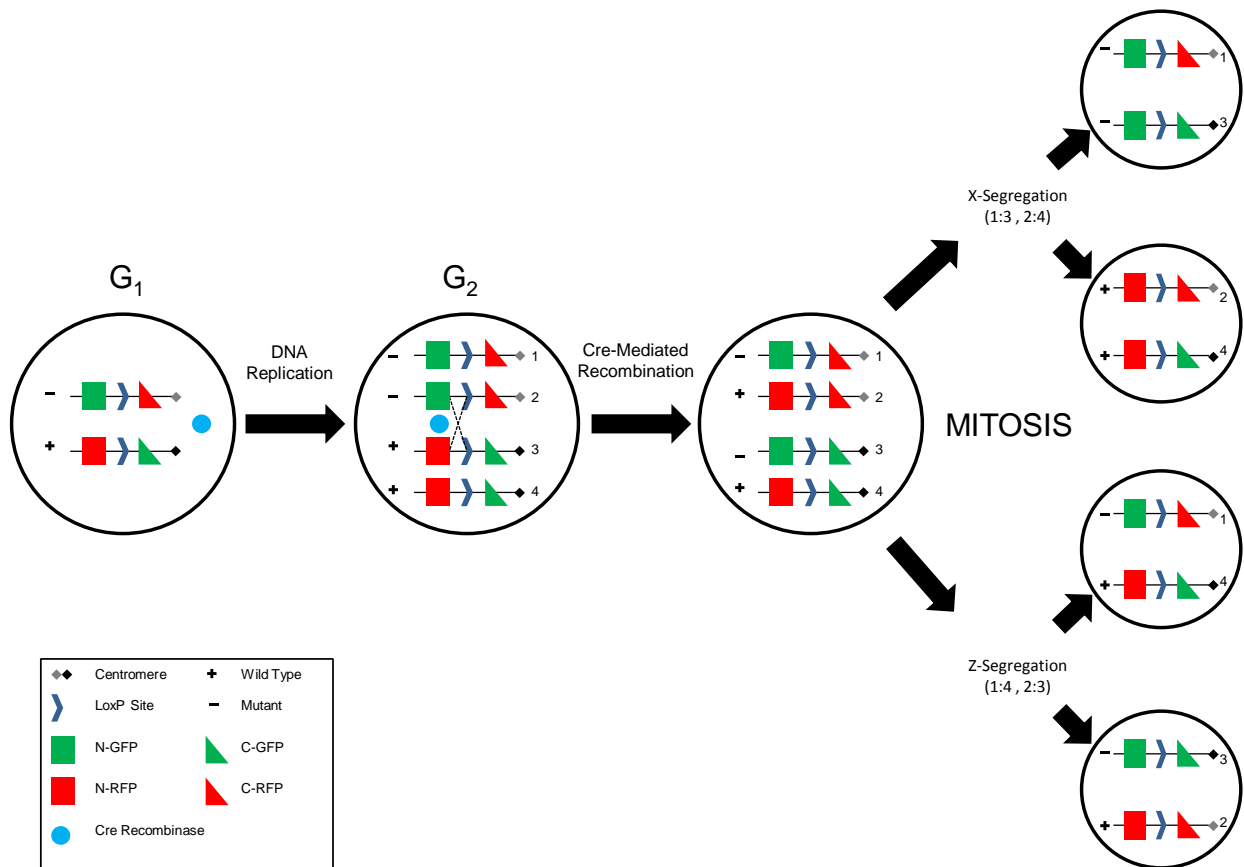


Figure 6. Methodology of MADM strategy given Cre-mediated G_2 recombination events. Following DNA synthesis in the S-phase, Cre targets LoxP sites to direct an interchromosomal recombination event. Subsequent removal of introns and X-segregation of chromosomes during mitosis generates singly labeled cells heterozygous for either GFP or RFP. Furthermore, fluorescently labeled daughter cells can now be identified by their genotype given the MADM scheme is arranged in conjunction with the respective gene knockout. Z-segregation results in colorless (no functional protein sequence) and double-labeled progeny.

In a MADM cell, the Cre-mediated recombination can occur at two points; G_0/G_1 and postsynthesis at G_2 . Once the recombination takes place, expression of the fluorescent proteins is not interrupted as the intron containing the LoxP site is removed through subsequent RNA splicing. Hence, the complete and functional protein sequences for either GFP or RFP seen in the third phase of figure 6. In the first instance, recombination occurring post-mitotically at G_0 or in the G_1 phase will always result in the restoration of both GFP and RFP sequences residing in the same cell leading to simultaneous green and red fluorescence. These double colored cells as noted in figure 7 appear yellow. On the other hand, if recombination were to occur after DNA synthesis at G_2 , the fluorescence seen from the successfully recombined cells is dependent upon the type of segregation the chromosomes follow.

As the last phase of figure 6 displays, X-segregation of chromosomes results in daughter cells that contain one recombinant chromatid and one unaltered chromatid each. On the other hand, Z-segregation of chromosomes results in one daughter cell containing both recombinant chromatids with the other having the non-recombinant chromatids (Stern, 1936; Chua and Jinks-Robertson, 1991). With respect to the MADM scheme where recombination occurs during G_2 , X-segregation reveals two daughter cells expressing only one of the two fluorescent proteins because the other chromosome does not host a functional protein sequence. Therefore, there will be one daughter cell that appears green and the other red under fluorescent microscopy, after X-segregation. On the other hand, Z-segregation results in one daughter cell containing the chromatids that have the functional GFP and RFP protein sequences. Again, these double colored cells appear yellow. The other daughter cell post-Z-segregation will house the chromatids that were not involved in Cre-mediated recombination. Therefore, no functional

protein sequences were produced, and the cell remains colorless. Figures 6 and 7 illustrate these outcomes further.

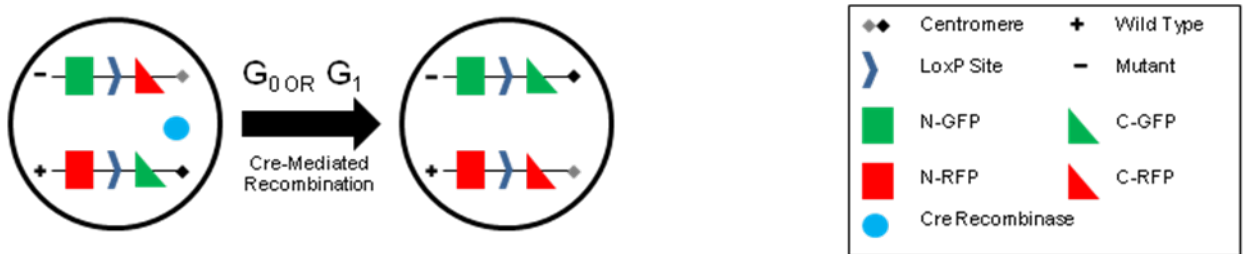


Figure 7. Methodology of MADM strategy given Cre-mediated G₀/G₁ recombination events. Cre-mediated recombination occurring in post-mitotic cells (G₀) or in G₁-phase will always generate daughter cells containing both the GFP and RFP protein sequences. Appearing yellow under fluorescence microscopy, these cells cannot be used for mosaic analysis because the true genotype of the daughter cell postrecombination is unable to be determined.

In the following experiments we show successful generation of MADM mice expressing two types of Cre strains in conjunction with a progenitor cell line. First, we have applied the MADM scheme around the aforementioned candidate progenitor K14 (K14-Cre). Secondly the Cre strain expressing hypoxanthine phosphoribosultransferase (Hprt-Cre) will be analyzed alongside K14-Cre. Hprt is ubiquitously expressed in all cells and will provide an unbiased approach to our clonal analysis seeing as all potential progenitor cell lines to the taste bud are ultimately involved. Visualizing taste buds from the CVP, we provide examples of all possible types of Cre-mediated interchromosomal recombination events. Furthermore, we begin the

initial studies in determining progenitor cell potency as it pertains to the types of taste cells produced. This is achieved using co-immunolabeling studies in which MADM-labeled cells in CVP tissue sections are subjected to immunohistochemical analyses to label functional taste cell types. Positive co-expression of MADM-labeled cells with those of functional taste cell types will indicate that the identified cell was derived from one of our progenitor cell lines.

MATERIALS AND METHODS

Mice and Genotyping

MADM mice were obtained from The Jackson Laboratory. Mice heterozygous for either the GR or RG transgenes were bred to obtain homozygous progeny. Homozygous RG mice were then mated with homozygous Cre-expressing mice (also from The Jackson Laboratory) to obtain progeny that were heterozygous for both RG and Cre. The latter animals were finally bred with homozygous GR mice to ultimately give rise to the experimental mice genotype. This contains reciprocally chimeric RG and GR inserts on homologous chromosomes along with heterozygous expression of the respective Cre-driver. These experimental mice, referred to as WT-MADM, were genotyped by PCR from snippets of tail taken from mice at approximately 3 weeks of age. Genomic DNA was extracted, purified, and amplified using the DNeasy Tissue Kit (Qiagen Inc., Valencia, CA) and construct insert-specific primers. Rosa10 (5'-CTC TGC TGC CTC CTG GCT TCT-3') and Rosa11 (5'-CGA GGC GGA TCA CAA GCA ATA-3') primers were used to detect and amplify a 330 bp fragment from wild-type alleles, while the Rosa10 and Rosa4 (5'-TCA ATG GGC GGG GGT CGT T-3') primers identify a 250 bp fragment from the knock-in cassette for MADM mice. K14-Cre transgene presence was

identified by primers (5'-TTC CTC AGG AGT GTC TTC GC-3') and (5'-GTC CAT GTC CTT CCT GAA GC-3') to amplify a product of 494 bp while Hprt-Cre primers included (5'-GCG GTC TGG CAG TAA AAA CTA TC-3') and (5'-GTG AAA CAG CAT TGC TGT CAC TT-3') to yield amplified products of 173 and 102 bp (transgene and wild-type alleles, respectively). PCR for all of these scenarios was performed for 32 cycles under these conditions: 94° (20 minutes), 58° (25 minutes), and 72° (45 minutes). All PCR products were subjected to gel electrophoresis on a 2% agarose gel and visualized under ultraviolet light post-Sybr Gold staining (Molecular Probes, Eugene, OR). The breeding scheme is outlined in figure 8.

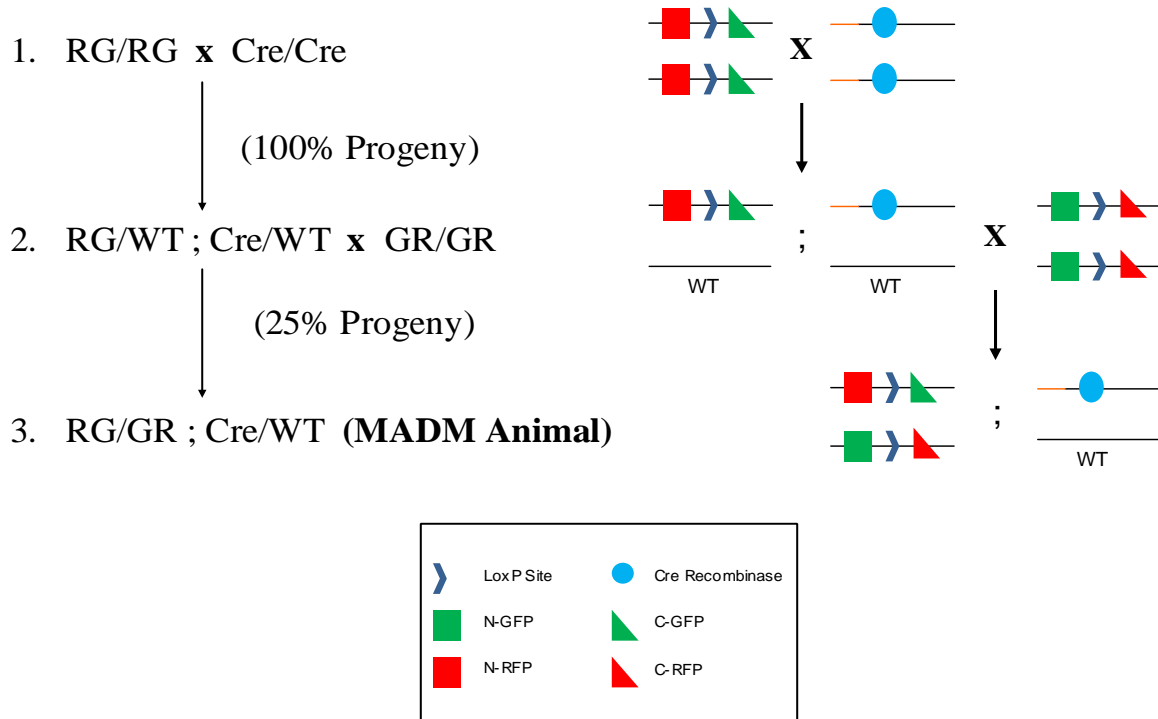


Figure 8. MADM breeding scheme. The first round of breeding is between mice homozygous for the RG strain and mice homozygous for the respective Cre-recombinase strain. All of the progeny from this mating will be heterozygous for both RG and Cre. These progeny were then bred with mice homozygous for the GR strain to produce another generation of mice in which one-fourth of the progeny are expected to contain the experimental genotype. These MADM mice are reciprocally chimeric for the RG and GR constructs on homologous chromosomes along with heterozygous expression of the respective Cre-driver.

Preparation of Circumvallate Papillae Sections

MADM mice were euthanized by CO₂ asphyxiation, and tongue tissues were surgically extracted and trimmed down to only the portion of tissue containing the CVP. The CVP tissue was fixed at room temperature overnight in 4% paraformaldehyde (PFA) in PBS. The following day the CVP tissue was submitted to three 10 minute washes with PBS and left in fresh PBS overnight. Tissues were cryoprotected on the third day in steps of 10% sucrose (in PBS) for 12 hours at 4°C followed by 20% sucrose (in PBS) overnight at 4°C. The tissue was then embedded

in OCT and frozen in liquid nitrogen then stored at -70°C until sectioned. Sections ($25\mu\text{m}$) were cut on a cryostat microtome at -20°C , sequentially collected on gelatin-subbed slides, dried on a slide warmer at 37°C for at least 1 hour, and stored at -20°C until use for IHC.

MADM Immunohistochemistry

Tongue tissue containing the CVP was surgically removed and prepared for sectioning as previously explained. Slides containing serial CVP sections first underwent antigen retrieval in 10 mM citrate buffer (pH 6.0, 15 min, 97°C) and were then incubated in 10% normal serum in standard incubation buffer, followed by overnight incubation at 4°C with combined primary antibodies, chicken polyclonal anti-GFP (1:500; Aves Labs, Tigard, OR) and rabbit polyclonal anti-c-Myc (1:200; Novus Biologicals, Littleton, CO). Immunodetection of anti-GFP was accomplished with an FITC-conjugated anti-chicken secondary antibody (1:200; Jackson ImmunoResearch Laboratories, West Grove, PA). An Alexa Fluor 555 conjugated anti-rabbit secondary (1:400) was used to detect c-Myc labeling. After washing, functional taste cell type co-labeling began by blocking with normal serum and incubating overnight in primary antibody for either PLC β -2 (1:1000) or SNAP-25 (1:500). PLC β -2 labeling was identified by biotinylated secondary antibody (1:400) at room temperature for 2 hours and streptavidin-conjugated Alexa Fluor 647 (1:600) for 1 hour. Visualization of SNAP-25 labeling was achieved by a secondary antibody directly conjugated to Alexa Fluor 647 (1:400) for 2 hours.

Confocal Microscopy and Data Analysis

MADM labeled sections were visualized in a similar manner as in the p27^{Kip1} study described above. CVP sections were visualized using the Leica SP confocal laser scanning microscope with 20X infinity-corrected objective. Series of high and low power optical sections were obtained through the z-axis and constructed to form a maximum projection as previously described.

RESULTS

Initial experiments were conducted to test the effectiveness of the MADM technique for study of taste cell turnover. For this study two Cre-recombinase enzyme drivers were used, K14-Cre and Hprt-Cre. Our results show that in mice from both Cre-recombinase lines, we initially see native GFP fluorescence, signifying a successful recombination event. Figure 9 illustrates a series of CVP sections providing examples of the native GFP fluorescence as seen in mice from both Cre-driver models prior to further immunohistochemical processing. In both Cre lines we see discrete single cells being labeled with the native GFP within the taste bud. While their morphology suggest that these are likely taste cells of a functional subtype, further immunohistochemical processing will be needed to confirm this. Also to note are the sites of GFP labeling that occur outside the taste buds. In some instances, the labeling occurs in cells of the immediate area surrounding the taste buds, likely to be perigemmal keratinocytes. Some flattened cells at the edge of the CVP cleft are also noticeably fluorescing GFP. These cells are likely the aforementioned perigemmal keratinocytes proceeding towards desquamation. Initial

cell counts indicate approximately a 3.5-fold greater number of MADM-labeled cells in the Hprt cell line as compared to the Krt14 model.

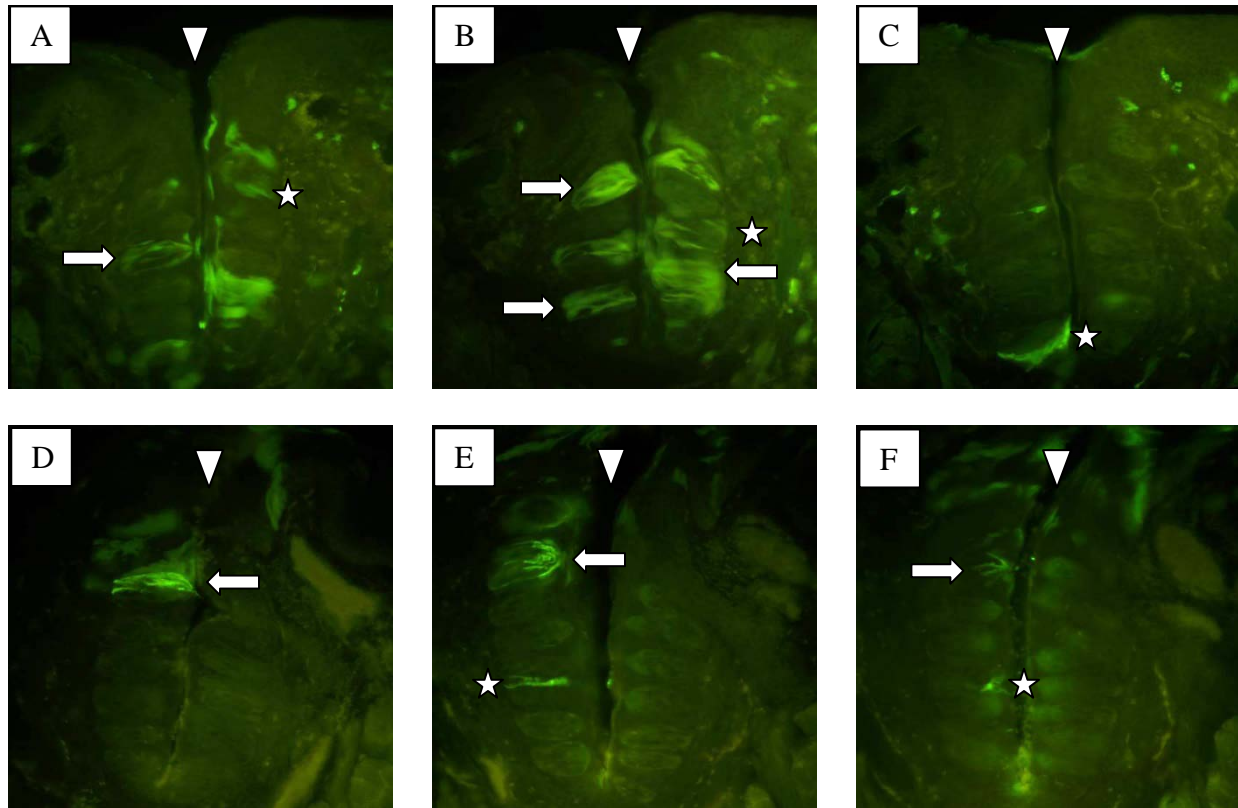


Figure 9. Fluorescent stereoscopy images visualizing MADM recombination events. These frames highlight examples of successful Cre-mediated recombination events in taste buds, evidenced by native GFP fluorescence. Both Cre-recombinase cell lines give rise to elongate and isolated GFP-fluorescing cells within the taste bud. One cleft of the CVP is identified in each frame by the arrowhead. Arrows illustrate instances in which multiple taste cells are labeled; whereas the stars highlight occasions where only one or two cells in the taste bud express GFP. As a whole, the Hprt-Cre driver (A-C) proves to be a more efficient than the K14-Cre driver (D-F) in the production of recombination events as shown by the higher incidences of GFP expression in taste buds.

As referred to earlier, MADM recombination results in the construction of two full proteins, GFP and RFP. As the technique currently stands, the native GFP can easily be seen under fluorescence microscopy. However, RFP is too dim to be visualized without enhancement. In order to locate MADM-labeled cells containing RFP, a c-Myc tag was incorporated just upstream of the RFP sequence to serve as an identifying marker. Therefore, all RFP-labeled cells were visualized using an anti-c-Myc antibody (Zong et al, 2005). In order to sufficiently label the RFP-containing cells, we found that it was necessary to perform antigen retrieval on the tissue prior to application of the primary antibody to c-Myc. While this distinctly identifies RFP-labeled cells, the antigen retrieval in turn partially destroys the native GFP fluorescence previously seen. Therefore, in conjunction with the anti-c-Myc antibody to identify cells containing RFP, an anti-GFP antibody was used to enhance cells containing the functional GFP sequence.

Initial double-labeling for GFP and RFP resulted in clear relabeling of GFP containing cells, but RFP labeling proved to be a little hazy (data not shown). It could be noticed that the c-Myc antibody was identifying areas of MADM recombination, but the precision of the labeling was not sufficient. In Zong's (2005) application of the c-Myc antibody to neurons, it was necessary to pre-absorb the antibody on mouse tissue that did not express the initial RG knock-in construct, as it also contains the c-Myc tag within it. This essentially "cleaned up" the antibody to allow for more defined visualization of RFP-containing cells due to a reduction of background labeling to surrounding mouse tissues. In the present experiments the c-Myc antibody used for RFP labeling was pre-absorbed on wild-type mouse cornea tissues for a minimum of 2 days. Figure 10 shows the final result from double-labeling with anti-GFP and the pre-absorbed anti-c-Myc antibodies. For both GFP and RFP-containing cells, we see similar characteristics amongst

cells as compared to CVP sections prior to immunohistochemical treatment. Distinct, elongated cells from within the taste buds and shorter cells outside the buds are labeled, indicating GFP and RFP presence. In addition, we also see an asymmetric division amongst the labeled cells evidenced by the inequality of the number of green versus red fluorescing cells seen in individual taste buds.

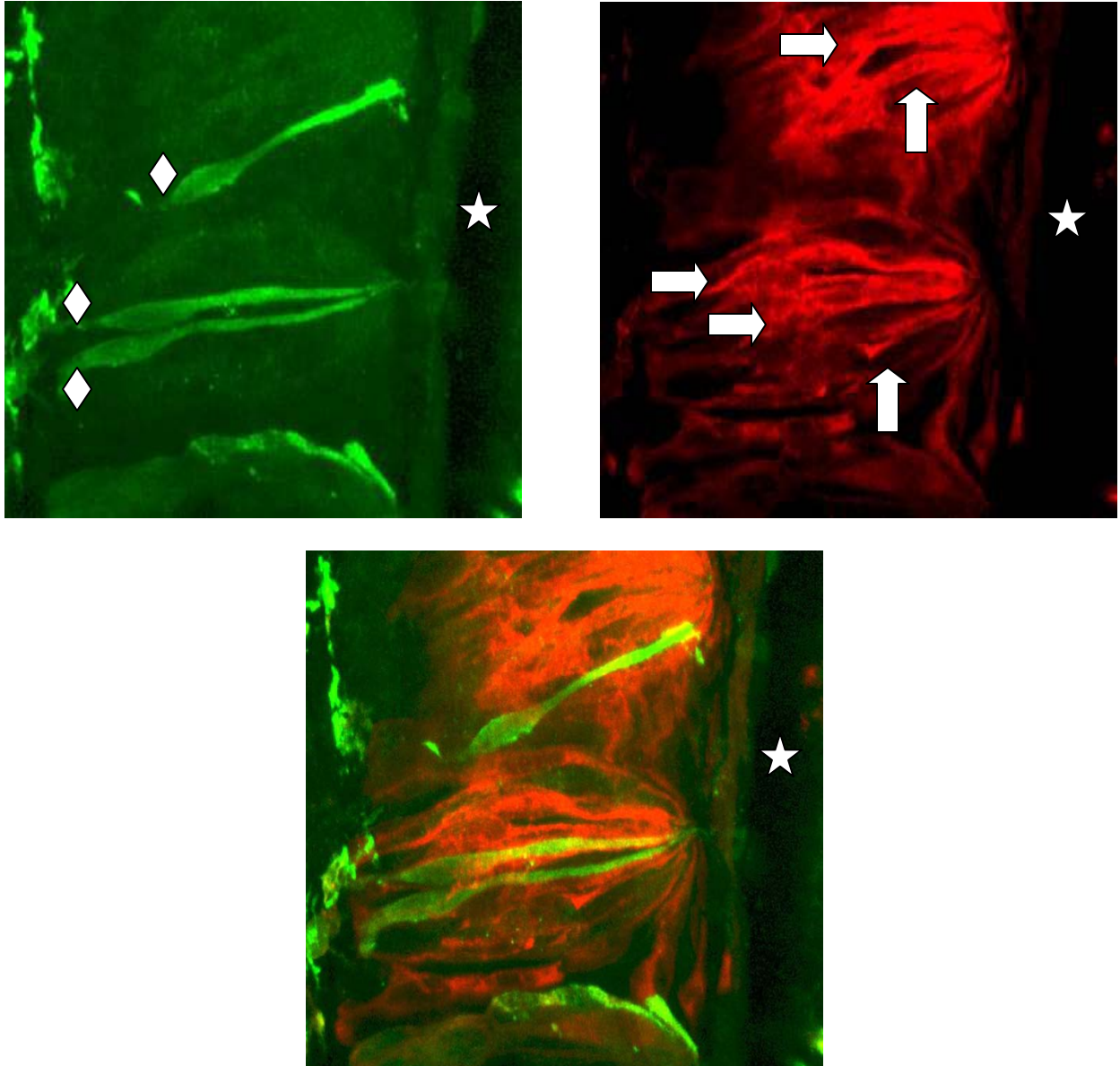


Figure 10. GFP and RFP labeled taste cells represents MADM recombination events. Maximum confocal projection images (25 μ m, 1 μ m step optical series) of GFP (green) and RFP (red) labeled taste cells in the CVP, identified using antibodies for GFP and c-Myc (RFP). Distinct cell body labeling within the taste buds located left of the CVP cleft (star) is noticed for cells hosting either fluorophoric protein. Initial analyses of such images indicate a higher number of RFP labeled cells as compared to GFP. Asymmetry is noted in the top and middle taste buds as the number of GFP-labeled cells (diamond) is not equal to the number of RFP-labeled cells (arrows).

Our results up until this point demonstrate examples of MADM-labeled cells resulting from G2-X recombination events, where resultant progeny will either express GFP or RFP. As Zong and colleagues indicate, there is also the possibility for such recombination to occur at the G0/G1 phase of the cell cycle or for a separate chromosomal segregation pattern to occur after G2 recombination, identified as G2-Z (Zong et al. 2005). In either of the latter two scenarios, the subsequent daughter cells will either contain both GFP and RFP sequences, hence appearing yellow, or will remain unlabeled due to lack of a functional fluorescent protein construct. In our taste model progeny of such recombination are often seen within the same taste bud as cells from G2-X recombination events. However, it is not possible to determine whether these progeny are derived from G0/G1 or G2-Z recombination events. Nonetheless, we do see examples of these in both Hprt and Krt14 mouse models. Figure 11 provides an occurrence of all such recombination events in a mouse expressing the Krt14 driver. We see labeling similar to what has been shown in previous figures. In multiple taste buds elongated, single cells express either GFP or RFP. We also notice yellow cells within the taste bud, indicating that a recombination event other than G2-X took place. Once again, asymmetrical division appears to be taking place due to an imbalance in fluorescent cell types in the asterisked taste bud.

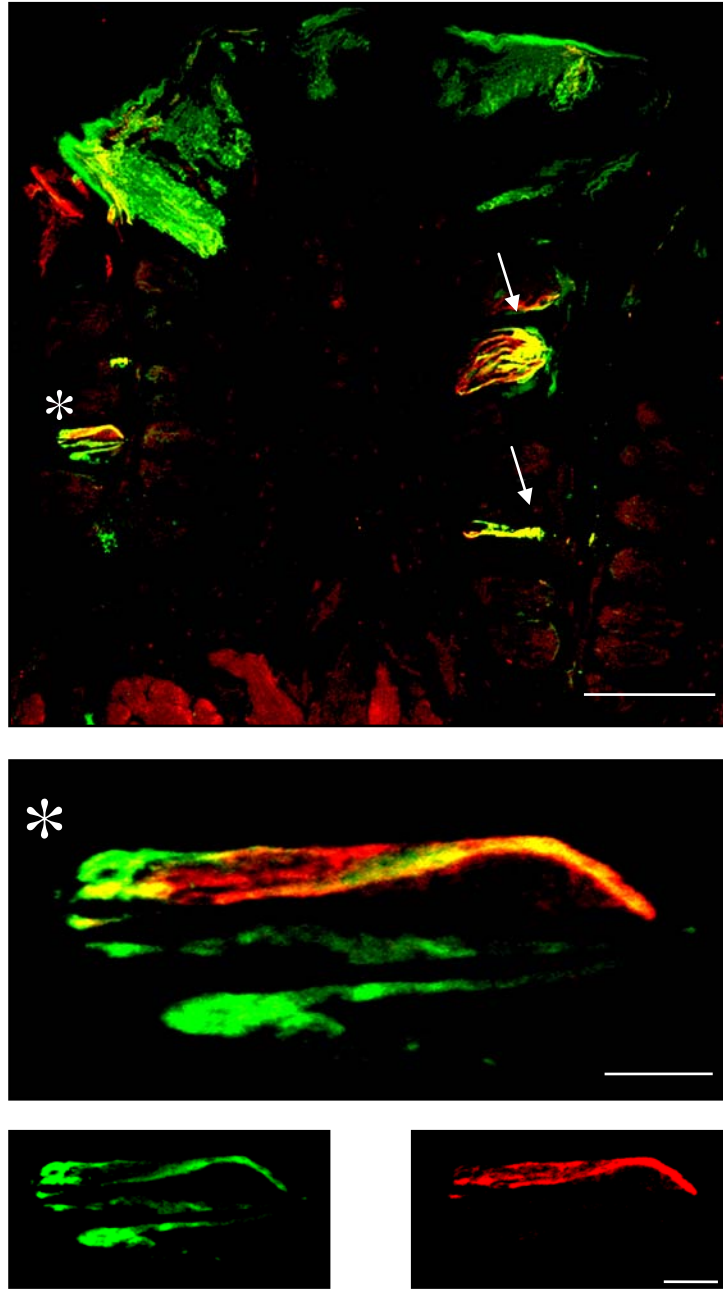


Figure 11. GFP and RFP labeled taste cells in mouse expressing K14-Cre recombinase. (Top) Confocal maximum projection image (25 μ m, 1 μ m step optical series) of CVP section double-labeled for anti-GFP and anti-c-Myc. Taste buds with multiple recombination events evidenced by single cells expressing GFP (green), RFP (red), or both (yellow) indicated with arrows (Scale Bar = 100 μ m). (Middle) Confocal projection image of asterisked taste bud visualized at high power (Scale Bar = 10 μ m). A minimum of two recombination events are noted here due to single GFP-labeled cells with an absence of coinciding RFP expressing cells as well as a cell expressing both GFP and RFP. Analysis at 1 μ m intervals confirms dual expression. (Bottom) The individual confocal projection images of GFP (left) and RFP (right), which are overlaid above at higher magnification. (Scale Bar = 10 μ m)

Similar to the previous Krt14 images, the Hprt line also shows evidence of varying types of recombination events; however, more frequent in number. Figure 12 illustrates these events. We see multiple taste buds within the CVP containing elongated cells that appear yellow, indicating either G₂-Z or G₀/G₁ Cre-mediated recombination events. However, it is also important to note the asterisked taste bud in which all three types of recombination events potentially occur. Evident are two GFP-expressing cells along with a single RFP-expressing cell, which are only possible from G₂-X recombination events. We also notice what appears to be a portion of a yellow cell in the upper left portion of the high-power, asterisked taste bud. Again, asymmetric cell division appears to be occurring as evidenced by differences in fluorescent cell number.

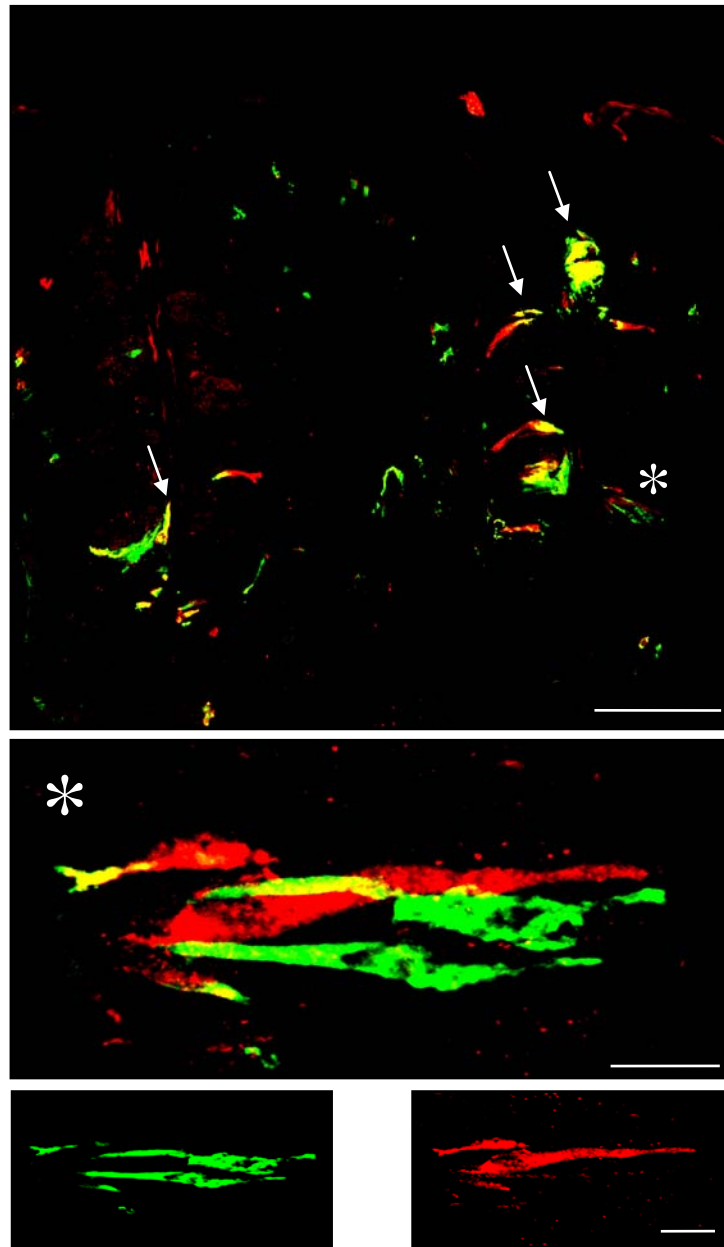


Figure 12. GFP and RFP labeled taste cells in mice expressing Hprt-Cre recombinase. (Top) Confocal maximum projection image (25 μ m, 1 μ m step optical series) of CVP double-labeled for anti-GFP and anti-c-Myc in mouse expressing Hprt-Cre recombinase. Taste buds highlighting recombination events at the G2-Z or G0/G1 phase of the cell cycle (yellow) indicated with arrows (Scale Bar = 100 μ m). (Middle) Confocal projection image of asterisked taste bud visualized at high power (Scale Bar = 10 μ m). Individual taste cells expressing either GFP or RFP are seen distinct from one another, indicating G2-X recombination from at least one Hprt-expressing progenitor cell. Analysis at 1 μ m intervals confirms fluorophoric protein expression in separate, isolated cells. (Bottom) Individualized confocal projection images of GFP (left) and RFP (right) from which the overlay image (above, at higher magnification) was constructed. (Scale Bar = 10 μ m).

Thus, analyses of GFP and RFP labeling in taste buds from the CVP in animals expressing both Cre-drivers show labeling of individual taste cells with morphologies similar to that of functional taste cells. In order to confirm that the labeled cells within the taste bud are legitimate functional cell types, we carried out further immunohistochemical labeling. We have shown thus far that at least one subtype of taste cell is labeled in MADM recombination events. Figure 13 provides multiple occurrences in which Type II cells (identified with anti-PLC β -2, magenta) in an animal expressing the K14-Cre recombinase line is also co-labeled with GFP (identified with anti-GFP, green) and RFP (identified with anti-c-Myc, red). This is indicative of Cre-mediated recombination events occurring at either the G₀/G₁ or G₂-Z phase of the cell cycle. In the same section, we are also able to identify Type II cells that do not co-label with MADM labeled cells. These singly labeled Type II cells may represent the colorless sister cells resulting from a G₂-Z MADM recombination event. On the other hand, these cells may not have derived from K14-expressing progenitor pool or undergone recombination at all.

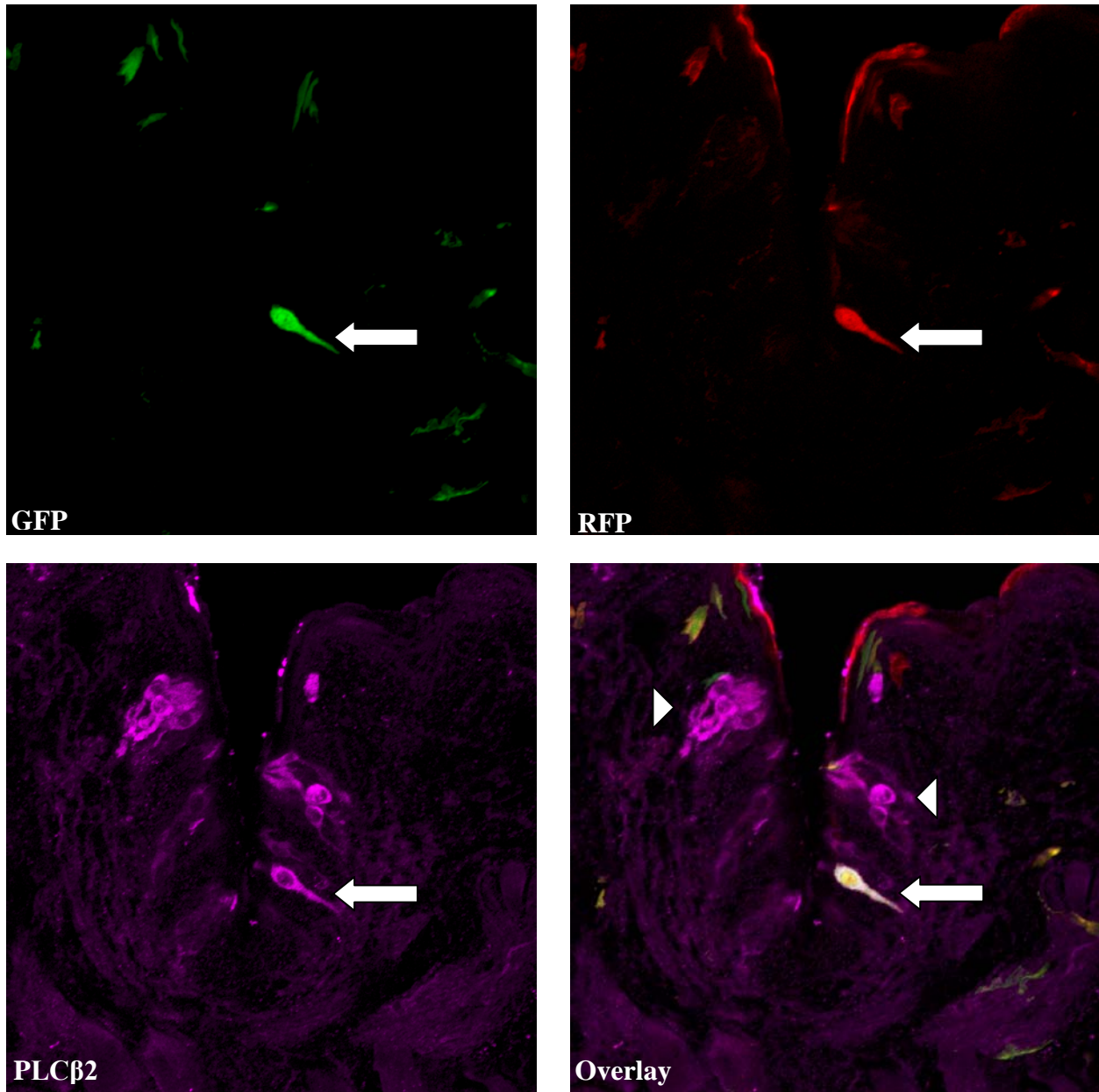


Figure 13. Type II cells are labeled by MADM in mice expressing the K14-Cre driver. In the upper row we see confocal maximum projection images (25 μ m, 1 μ m step optical series) for GFP (left) and RFP (right). The bottom row shows the same tissue immunolabeled for Type II cells with PLC β 2 (left) as well as the overlay (right) of the three aforementioned images. Notice the Type II cell being positively co-labeled for cells that have undergone MADM recombination events (arrows). This is indicative of a MADM recombination event occurring during either the G₀/G₁ or G₂-Z phase. Also of note, the singly labeled Type II cells in the overlay image (arrowheads) may represent the sister progeny produced from G₂-Z recombination in the MADM scheme. Furthermore, these same cells may not have undergone MADM recombination or could have possibly been produced from a progenitor cell population not expressing K14.

In addition, we also show that cells other than Type II cells are produced by the K14-expressing Cre driver. Figure 14 displays an isolated occurrence of a single cell spanning the length of a taste bud that has been labeled by a MADM recombination event but does not express PLC β 2, indicating that it is a taste cell other than Type II. Once again, the single cell appears yellow, demonstrating either a G₀/G₁ or G₂-Z MADM recombination event. More immunophenotyping experiments need to be carried out to make sound conclusions on the potency of the K14-Cre driver in their role of maintenance of the taste bud. Nonetheless, it appears that the K14-expressing progenitor pool population in fact gives rise cells that mature into taste cells of more than one functional subtype

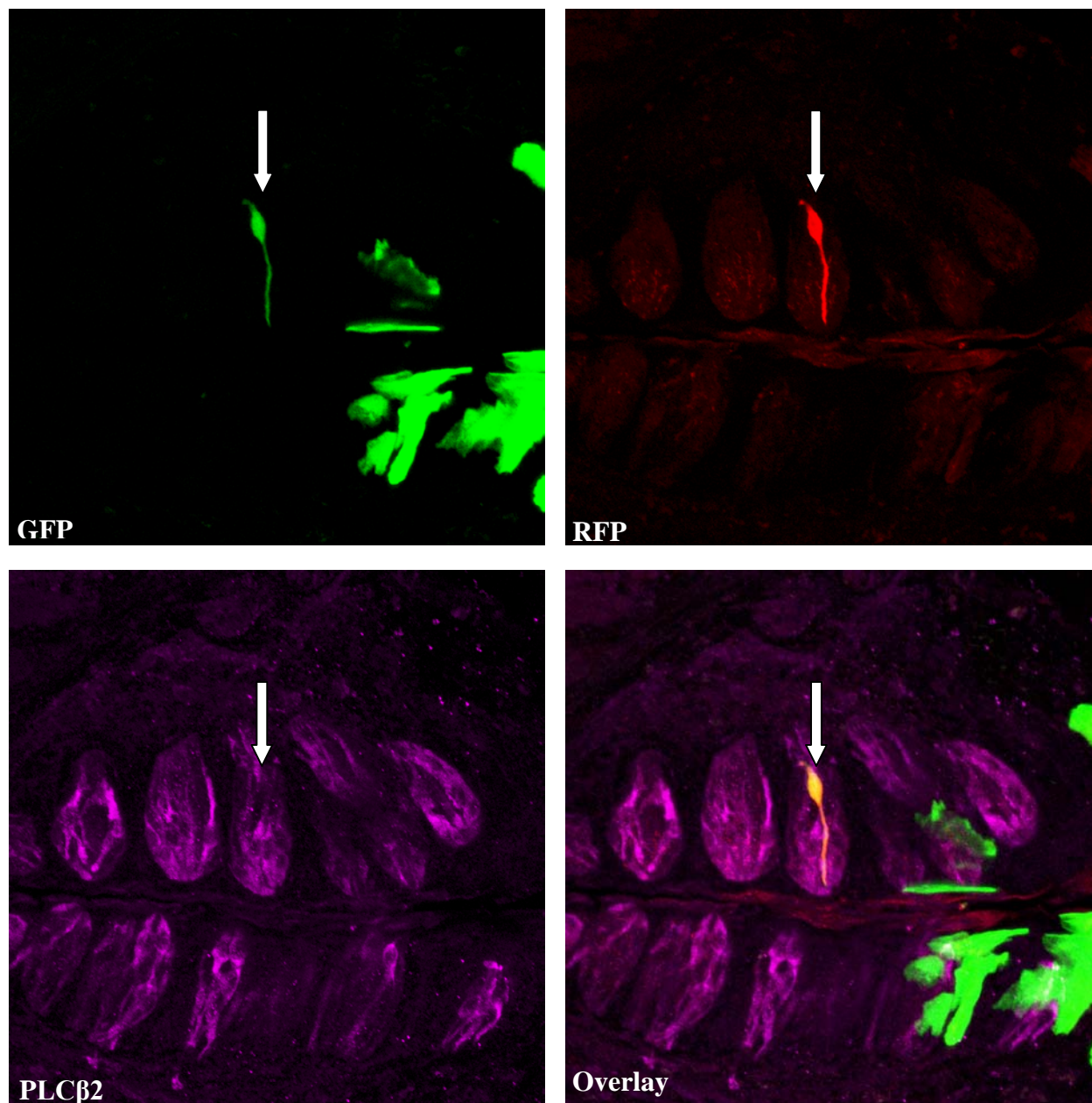


Figure 14. MADM labels taste cells other than Type II in mice expressing the K14-Cre driver. In the upper row, we see confocal maximum projection images (25 μ m, 1 μ m step optical series) for GFP (left, green), RFP (right, red). The bottom row shows the same tissue immunolabeled for Type II cells with PLC β 2 (left, magenta) as well as the overlay (right) of the three aforementioned images. Notice the isolated occurrence of a singly labeled MADM cell that did not co-label with the marker expressed for Type II taste cells (arrows). This yellow cell is indicative of a MADM recombination event occurring during either the G₀/G₁ or G₂-Z phase. Furthermore, this illustrates that the K14-expressing progenitor cell line can give rise to taste cells that mature into more than one functional subtype.

DISCUSSION

In this study, we investigated the maintenance of taste buds through obtaining a better understanding about the potency of progenitor cell lines that have been previously shown to supply cells to the taste bud. Using MADM, we were able to provide a true clonal analysis of daughter cells from both the K14 and Hprt-Cre progenitor cell lines. While more data is needed to confirm these results, we show that the K14-expressing cells previously described by Asano-Miyoshi definitely give rise to progeny that ultimately mature into functional Type II taste cells. We have just begun an analysis on the Type I and Type III cells, and results as of yet remain inconclusive. Although the MADM technique provides high-impact, single-celled resolution of fluorescently labeled cells from the progenitor lines used, for the sake of establishing progenitor potency alone, it may be pertinent to complete another dispersed cell preparation with the taste buds obtained from MADM animals similar to that used in the p27^{Kip1} study. This will undoubtedly allow for us to immunophenotype the taste cells and analyze for co-labeling of functional taste cells with MADM cells that have undergone Cre-mediated DNA recombination and are now fluorescing. However, the dispersed cell approach takes away from the MADM technique's purpose in clonal analysis and lineage tracing of cells from their progenitors seeing as the taste bud is no longer in intact tongue tissue. Therefore, single clones cannot be identified if the cell dispersion technique is applied to the MADM animals.

Also with regards to the data seen in the MADM experiments, there appears to be some asymmetrical division seen in each of our examples that display GFP and RFP (Figures 10, 11, and 12). Again, more data needs to be obtained to confirm these initial findings, but our preliminary data indicates that there may not be an equal potential for expansion between sibling cells. This would make more sense in the scenario where we have incorporated the p27^{Kip1}-null

mutation into the MADM scheme in order to complete a mosaic analysis between wild-type and mutant cells within the microenvironment of the taste bud. This is discussed in greater detail later. For now, because the relative numbers of GFP- to RFP-labeled cells are fairly similar, it is a possibility that one or more of the fluorescently-labeled cells may have already undergone apoptosis. For instance, the uppermost taste bud in figure 10 displays clear asymmetry in that there is only one GFP-labeled cell and two or more RFP-labeled cells. Because the lifespan of a taste cell in the bud spans on average 10-14 days, we may have simply caught the taste cells for this particular specimen during the approximately four day lag. Also, it is possible that during tissue sectioning, a taste bud was sectioned in half. Therefore, the accompanying labeled sister cells are merely in adjacent sections not included in the data above. Finally, the bipotential division by the K14-expressing first noted by Okubo and his colleagues may be a factor in the noted asymmetry. Okubo recently showed that K14-expressing cells outside the taste bud can give rise to both functional taste cells and taste bud-surrounding keratinocytes (Okubo et al. 2009). If this is the case for the preceding data, then the labeled sister cell, a possible taste bud-surrounding keratinocyte, may have already migrated to the oral epithelial surface and undergone desquamation.

REFERENCES

- Chua P, Jinks-Robertson S. Segregation of Recombinant Chromatids Following Mitotic Crossing Over in Yeast. *Genetics*. 1991; 129: 359-369.
- Muzumdar MD, Luo L, Zong H. Modeling sporadic loss of heterozygosity in mice by using mosaic analysis with double markers (MADM). *Proc. Natl. Acad. Sci. USA* 2007; 104: 4495-4500.
- Okubo T, Clark C, Hogan BL. Cell lineage mapping of taste bud cells and keratinocytes in the mouse tongue and soft palate. *Stem Cells*. 2009; 27: 442-450
- Stern C. Somatic crossing over and segregation in *Drosophila melanogaster*. *Genetics*. 1936; 21: 625-730.
- Sternberg N, Hamilton D. Bacteriophage P1 site-specific recombination. I. Recombination between LoxP sites. *J. Mol. Biol.* 1981; 150: 467-486.
- Stricklett PK, Nelson RD, Kohan DE. The Cre/LoxP system and gene targeting in the kidney. *Am. J. Physiol.* 1999; 276: 651-657.
- Zong H, Espinosa JS, Su HH, Muzumdar MD, Luo L. Mosaic analysis with double markers in mice. *Cell*. 2005; 121: 479-492.

CHAPTER 4

FUTURE DIRECTIONS

In conjunction with further investigating the progenitor potency of K14 in supplying taste cells, lineage tracing analysis can be better studied with the incorporation of an inducible-Cre line. In this methodology the Cre-recombinase enzyme is fused with a truncated estrogen receptor (ER) that is sensitive to a drug called tamoxifen. This new Cre strain, now identified in the MADM system we are currently using as K14-CreER, allows for temporal regulation of expression of specific genes (Feil et al. 1997; Guo et al. 2002; Hayashi and McMahon, 2002; Shi and Bassnett, 2007). Prior to tamoxifen administration, the CreER recombinase remains sequestered in the cytoplasm because the estrogen receptor attached to Cre does not bind to the natural estradiol ligand present in the system. When tamoxifen is introduced, CreER recombinase becomes free from any inhibitory binding elements and is allowed to translocate into the nucleus of the cell (Feil et al. 1997). At this point the recombinase can now interact with the LoxP sites on the reciprocally chimeric MADM strains to induce the Cre-mediated interchromosomal recombination we seek. This will prove very advantageous to lineage tracing studies because birthdating of fluorescently labeled cells can be more closely pinpointed by the date of tamoxifen administration. At this point the lineage tracing study for K14-CreER mice is completed by giving an appropriate dosage of tamoxifen to a group of animals and sacrificing individuals at progressively longer timepoints, 3 days to 3 weeks, to process for IHC as previously described.

The ultimate goal is to have all of these components come together in future experiments so that we can use MADM to its fullest extent. First, as previously mentioned and figure 6 depicts, the MADM technique can be used to study gene function as it relates to the tracking of

single cells (Zong et al. 2005). In this case, four strains of mice are bred across three generations to produce progeny that are reciprocally chimeric for the RG and GR strains, heterozygous for the p27^{Kip1}-null allele (meiotically bred with the GR strain), and heterozygous for the Cre-recombinase enzyme (bred with the RG strain). The Cre-strain for these experimental animals can be interchanged with the CreER strain as well. Once the Cre-mediated DNA recombination occurs, singly fluorescent cells can now be genetically identified by their appearance. For the above breeding scheme, the daughter cells that fluoresce green will contain the p27^{Kip1}-null allele and red daughter cells will be wild-type. Now, not only can the progenitor potency of K14 be addressed in a temporal matter, but a true mosaic analysis for p27^{Kip1} function can now be completed in the taste bud environment. Both wild-type and mutant taste cells can be traced in synchrony with one another from the progenitor level to answer if p27^{Kip1} acts independently of taste bud precursor cells to impact the length of the cell cycle as well as timing cell cycle exit.

REFERENCES

- Asano-Miyoshi M, Hamamichi R, Emori Y. Cytokeratin 14 is expressed in immature cells in rat taste buds. *J. Mol. Hist.* 2008; 39: 193-99.
- Barlow LA, Northcutt RG. Embryonic origin of amphibian taste buds. *Dev. Biol.* 1995; 169: 273-285.
- Bartel DL, Sullivan SL, Lavoie EG, Sevigny J, Finger TE. Nucleoside triphosphate diphosphohydrolase-2 is the ecto-ATPase of type I cells in taste buds. *J. Comp. Neurol.* 2006; 497: 1-12.
- Beidler LM, Smallman RL. Renewal of cells within taste buds. *J. Cell Biol.* 1965; 27: 263-272.
- Chaudhari N, Roper S. The cell biology of taste: Cells, synapses, and signals in taste buds. *The Journal of Cell Biology.* 2010; 3: 285-296.
- Chua P, Jinks-Robertson S. Segregation of Recombinant Chromatids Following Mitotic Crossing Over in Yeast. *Genetics.* 1991; 129: 359-369.
- Clapp TR, Stone LM, Margolskee RF, Kinnamon SC. Immunocytochemical evidence for co-expression of type III IP3 receptor with signaling components of bitter taste transduction. *BMC Neurosci.* 2001; 2: 6.
- Clapp TR, Yang R, Stoick CL, Kinnamon SC and Kinnamon JC. Morphological characterization of rat taste receptor cells that express components of phospholipase C signaling pathway. *J. Comp. Neurol.* 2004; 468: 311-321.
- Clapp TR, Medler MF, Damak S, Margolskee RF, Kinnamon SC. Mouse taste cells with G protein-coupled taste receptors lack voltage-gated calcium channels and SNAP-25. *BMC Biol.* 2006; 4: 7.
- Conger AD, Wells MA. Radiation and aging effects on taste cell structure and function. *Radiat. Res.* 1969; 37: 31-49.
- DeFazio RA, Dvoryanchikov G, Maruyama Y, Kim JW, Pereira E, Roper SD, Chaudhari N. Separate populations of receptor cells and presynaptic cells in mouse taste buds. *J. Neurosci.* 2006; 26: 2227-2234.
- Delay RJ, Kinnamon JC, Roper SD. Ultrastructure of mouse vallate taste buds: II. *J. Comp. Neuro.* 1986; 253: 242-252.
- Drexler HG. Review of alterations of the cyclin-dependent kinase – inhibitor INK4 family gene p15, p16, p18, and p19 in human leukemia-lymphoma cells. *Leukemia.* 1998; 12: 845-859.

- Durand B, Fero ML, Roberts JM, Raff MC. p27^{Kip1} alters the response of cells to mitogen and is part of a cell intrinsic timer that arrests cell cycles and initiates differentiation. *Curr. Biol.* 1998; 8: 431-440.
- Durand B, Raff M. A cell-intrinsic timer that operates during oligodendrocyte development. *Bioessays.* 2000; 22(1): 64-71.
- Farbman AI. Renewal of taste bud cells in rat circumvallate papillae. *Cell Tissue Kinet.* 1980; 13: 349-357.
- Feil R, Wagner J, Metzger D, Chambon P. Regulation of Cre recombinase activity by mutated estrogen receptor ligand-binding domains. *Biochem. Biophys. Res. Commun.* 1997; 237: 752-757
- Finger TE, Danilova V, Barrows J, Bartel DL, Vigers AJ, Stone L, Hellekant G, Kinnamon SC. ATP signaling is crucial for communication from taste buds to gustatory nerves. *Science.* 2005; 310: 1495-1499.
- Guillemot F, Lo LC, Johnson JE, Auerbach A, Anderson DJ, Joyner AL. Mammalian achaete-scute homolog 1 is required for the early development of olfactory and autonomic neurons. *Cell.* 1993; 75: 463-476.
- Guo C, Yang W, Lobe C. A Cre Recombinase Transgene with Mosaic, Widespread Tamoxifen-Inducible Action. *Genesis.* 2002; 32: 8-18.
- Harrison TA, Adams LBS, Moore PD, Perna MK, Sword JD, Defoe DM. Accelerated turnover of taste bud cells in mice deficient for the cyclin-dependent kinase inhibitor p27^{Kip1}. *BMC Neurosci.* (submitted).
- Hayashi S, McMahon AP. Efficient recombination in diverse tissues by a tamoxifen inducible form of Cre: a tool for temporarily regulated gene activation/inactivation in the mouse. *Dev. Biol.* 2002; 244: 305-318.
- Hirota M, Ito T, Okudela K, Kawabe R, Hayashi H, Yazawa T, Fujita K, Kitamura H. Expression of cyclin-dependent kinase inhibitors in taste buds of mouse and hamster. *Tissue & Cell.* 2001; 33: 25-32.
- Huang YJ, Lu KS. TUNEL staining and electron microscopy studies of apoptotic changes in the guinea pig vallate taste cells after unilateral glossopharyngeal denervation. *Anat. Embryol.* 2001; 204: 493-501.
- Huang AL, Chen X, Hoon MA, Chandrashekar J, Guo W, Tränkner D, Ryba NJ, Zuker CS. The cells and logic for mammalian sour taste detection. *Nature.* 2006; 442: 934-938
- Huang YA, Maruyama Y, Stimac R, Roper SD. Presynaptic (Type III) cells in mouse taste buds sense sour (acid) taste. *J. Physiol.* 2008; 586: 2903-2912.

- Kinnamon JC, Dunlap M, Yang R. Synaptic Connections in Developing Adult Rat Taste Buds. *Chem. Senses*. 2005; 30-Supplemental 1: i60-i61.
- Lawton DM, Furness DN, Lindemann B, Hackney CM. Localization of the glutamate-aspartate transporter, GLAST, in rat taste buds. *Eur. J. Neurosci*. 2000; 12: 3163-3171.
- Lo LC, Johnson JE, Wuenschell CW, Saito T, Anderson DJ. Mammalian achaete-scute homolog 1 is transiently expressed by spatially restricted subsets of early neuroepithelial and neural crest cells. *Genes Dev*. 1991; 5: 1524-1537.
- Luo X, Okubo T, Randell S, Hogan BL. Culture of endodermal stem/progenitor cells of the mouse tongue. *In Vitro Cell Dev Biol Anim*. 2009; 45(1-2): 44-54.
- Medler KF, Margolskee RF, Kinnamon SC. Electrophysiological characterization of voltage-gated currents in defined taste cell types of mice. *J. Neurosci* 2003; 23: 2608-2617.
- Miura H, Kusakabe Y, Harada S. Cell lineage and differentiation in taste buds. *Arch. Histol. Cytol*. 2006; 69: 209-225.
- Miura H, Barlow LA. Taste bud regeneration and the search for taste progenitor cells. *Archives Italiennes de Biologie*. 2010; 148: 107-118.
- Miyoshi MA, Abe K, Emori Y. IP(3) receptor type 3 and PLCbeta2 are co-expressed with taste receptors T1R and T2R in rat taste bud cells. *Chem. Senses*. 2001; 26: 259-265
- Murray RG. The ultrastructure of taste buds. *The Ultrastructure of Sensory Organs*. Ed. I. Friedmann. North Holland, Amsterdam: 1973; 1-81.
- Muzumdar MD, Luo L, Zong H. Modeling sporadic loss of heterozygosity in mice by using mosaic analysis with double markers (MADM). *Proc. Natl. Acad. Sci. USA* 2007; 104: 4495-4500.
- Nakamura S, Kamakura T, Ookura T. Tongue epithelial KT-1 cell-cycle arrest by TGF-beta associated with induction of p21(Cip1) and p15 (Ink4b). *Cytotechnology*. 2009; 61(3): 109-16.
- Okubo T, Clark C, Hogan BL. Cell lineage mapping of taste bud cells and keratinocytes in the mouse tongue and soft palate. *Stem Cells*. 2009; 27: 442-450
- Ozdener H, Yee KK, Cao J, Brand JG, Teeter JH, Rawson NE. Characterization and Long-Term Maintenance of Rat Taste Cells in Culture. *Chem. Senses*. 2006; 31: 279-290.
- Pines J. Cyclins and cyclin-dependent kinases: take your partners. *Trends Biochem. Sci*. 1993; 18: 195-197.

- Pumplin DW, Yu C, Smith DV. Light and dark cells of rat vallate taste buds are morphologically distinct cell types. *J. Comp. Neurol.* 1997; 378: 389-410.
- Richter TA, Caicedo A, Roper SD. Sour taste stimuli evoke Ca^{2+} and pH responses in mouse taste cells. *J. Physiol.* 2003; 547: 475-483.
- Romanov RA, Kolesnikov SS. Electrophysiologically identified subpopulation of taste bud cells. *Neurosci. Lett.* 2006; 395: 249-254.
- Roper SD. Signal transduction and information processing in mammalian taste buds. *Pflugers Arch.* 2007; 454: 759-776.
- Sherr CJ. D-type cyclins. *Trends Biochem Sci.* 1995; 20(5): 187-90.
- Sherr CJ, Roberts JM. CDK inhibitors: positive and negative regulators of G_1 -phase progression. *Genes & Development.* 1999; 13: 1501-1512.
- Shi Y, Bassnett S. Inducible gene expression in the lens using tamoxifen and a GFP reporter. *Experimental Eye Research.* 2007; 85: 732-737.
- Stern C. Somatic crossing over and segregation in *Drosophila melanogaster*. *Genetics.* 1936; 21: 625-730.
- Sternberg N, Hamilton D. Bacteriophage P1 site-specific recombination. I. Recombination between *LoxP* sites. *J. Mol. Biol.* 1981; 150: 467-486.
- Stone LM, Finger TE, Tam PPL, Tan SS. Taste receptor cells arise from local epithelium, not neurogenic ectoderm. *Proc. Natl. Acad. Sci.* 1995; 92: 1916-1920.
- Stone LM, Tan SS, Tam PPL, Finger TE. Analysis of cell lineage relationships in taste buds. *J. Neurosci.* 2002; 22: 4522-4529.
- Stricklett PK, Nelson RD, Kohan DE. The Cre/*LoxP* system and gene targeting in the kidney. *Am. J. Physiol.* 1999; 276: 651-657.
- Sullivan JM, Alexander AB, Oleskevich S. Stem and progenitor cell compartments within adult mouse taste buds. *European Journal of Neuroscience.* 2010; 31: 1549-1560.
- Takeda M, Suzuki Y, Obara N, Nagai Y. Apoptosis in mouse taste buds after denervation. *Cell Tissue Res.* 1996; 286: 55-62.
- Takeda M, Suzuki Y, Obara N, Nagai Y. Induction of apoptosis by colchicine in taste bud and epithelial cells of the mouse circumvallate papillae. *Cell Tissue Res.* 2000; 302: 391-395.

- Thirumangalathu S, Harlow DE, Driskell AL, Krimm RF, Barlow LA. Fate mapping of mammalian embryonic taste bud progenitors. *Development*. 2009; 136: 1519-1528.
- Ueda K, Ichimori Y, Maruyama H, Murakami Y, Fujii M, Honma S, Wakisaka, S. Cell-type specific occurrence of apoptosis in taste buds of the rat circumvallate papilla. *Arch. Histol. Cytol.* 2008; 71(1): 59-67.
- Yang R, Crowley HH, Rock ME, Kinnamon JC. Taste cells with synapses in rat circumvallate papillae display SNAP-25-like immunoreactivity. *J. Comp. Neurol.* 2000; 424: 205-215.
- Zong H, Espinosa JS, Su HH, Muzumdar MD, Luo L. Mosaic analysis with double markers in mice. *Cell*. 2005; 121: 479-492.

VITA

PRESTON D. MOORE

- Personal Data: Date of Birth: June 16, 1986
Place of Birth: Newport News, Virginia
Marital Status: Single
- Education: Public Schools, Jackson, Tennessee
B.S. Biology, University of Tennessee, Knoxville,
Tennessee 2008
M.S. Biomedical Sciences, East Tennessee State
University, Johnson City, Tennessee 2010
- Publications: Harrison, T.A., Adams, L.B.S., Moore, P.D., Perna, M.K.,
Sword, J.D., Defoe, D.M. Accelerated turnover of taste
bud cells in mice deficient for the cyclin-dependent
kinase inhibitor p27^{Kip1}. *BMC Neurosci*. Submitted for
publication.
- Presentations: “Mosaic Analysis with Double Markers (MADM) as
Method to Map Cell Fates in Adult Mouse Taste
Buds”. Poster Presentation. Association for
Chemoreception Sciences (AChemS) Annual Meeting.
St. Pete Beach, FL. April 2010.

“Mosaic Analysis with Double Markers (MADM) as a
Method to Map Cell Fates in Adult Mouse Taste Buds”
Poster Presentation. Appalachian Student Research
Forum. East Tennessee State University. Johnson City,
TN. April 2010.
- Honors and Awards: James H. Quillen Scholar. East Tennessee State University.
Johnson City, TN. August 2009

2nd Place Poster Presentation, First and Second Year
Graduate Students in the Arts & Humanities and
Biomedical Science Division. Appalachian Student
Research Forum. East Tennessee State University.
Johnson City, TN. April 2010.